Hemodynamics of endoscopic imaging of Chronic Total Occlusions

Syed Faisal

A thesis
submitted in partial fulfillment of the
requirements for the degree of

Master of Science in Mechanical Engineering

University of Washington
2018

Committee:
Alberto Aliseda
Eric Seibel
James Riley

Program Authorized to Offer Degree:
Mechanical Engineering

University of Washington

Abstract

Optimization study of saline flushing in endoscopic diagnosis of CTOs using CFD

Syed Faisal

Chair of the Supervisory Committee:
Dr. Alberto Aliseda
Mechanical Engineering

This thesis investigates the fluid dynamics of saline flushing in endovascular catheters used in the treatment and diagnosis of chronic total occlusions (CTOs) in arteries. Using computational fluid simulations different designs of catheters are studied to understand and optimize parameters involved in flushing blood from the lumen space between the catheter tip and the CTO. Simple injection catheters are studied initially, and, in the interest of improving the catheter functionality, design modifications are made to the catheter. A suction lumen is introduced and its influence is investigated while testing different shapes and relative locations of the two lumens (injection and suction) in the catheter. The simulations are improved by introducing a pulsatile external blood pressure from the heart beat, different arterial radii and curvature in the artery to explore the different physical phenomena that could affect the performance of the catheter. Various plaque buildup and morphologies are investigated to test the viability of the catheter design. A new and improved method of saline injection, suction and control, which helps avoid risk of catheter failure and injury to the patient, is proposed. An optical analysis is performed to provide confirm

clearance of blood obtained in simulations. Analyzing the physical variables involved in the medical procedure, such as injection pressure and time to clear the lumen for optical transparency, as done in this thesis, helps recommend new and improved designs for catheters and can be used to reduced risk and improve success rates associated with the technique.

TABLE OF CONTENTS

Page

LIST OF FIGURES

LIST OF TABLES

ACKNOWLEDGMENTS

Over the course of two years, I had the incredible opportunity to work with Dr. Alberto Aliseda, who took me under his tutelage for which I am deeply grateful. From helping me acclimatize with the education system in the United States of America, to teaching me industry standards employed in research, he has been invaluable as a mentor to me. I thank Dr. Eric Seibel, whose ingenious ideas and vision, created a platform for me to work and provided me with the opportunity that led to this research. I also thank Dr. James Riley for assisting me in my research as well as teaching me the tools I need for this work. I am indebted to my wonderful parents who have been supporting me, blessing me with their wisdom, and helping me achieve everything in my life. My family and friends who've helped me in my times of difficulty, for which I am grateful. I thank my peers and colleagues working in our lab, from whom I sought help and guidance in working on my thesis and my research, and were always readily available for whenever I needed them.

DEDICATION

To my dear mother and father,

whose continuous sacrifice inspires me

to keep contributing in making a difference.

And to my loving family and friends who helped me in achieving my dream.

Chapter 1

INTRODUCTION

1.1 Cardiovascular Diseases

Cardiovascular diseases occur within the circulatory system of the human body, namely, the heart, blood vessels, and blood. Cardiovascular disease continues to be the leading cause of death worldwide with mortality rates estimated to increase by thirty six percent by 2030.[1] The heart and its vessels are affected by numerous problems many of which are caused due to an underlying process called atherosclerosis. Atherosclerosis is an illness wherein the walls of the blood vessel thicken due to the development of the plaque in them. This plaque built up reduces the lumen of the arteries, resulting in decreased blood flow.[2] Inadequate blood flow deprives the heart and other organs from critical nutrients and oxygen which are required to maintain appropriate function. The narrowed arteries and the subsequent low blood flow has downstream effects on different parts of the human body. In certain cases a complete obstruction of blood flow caused by the decrease in arterial lumen can result in a heart attack (myocardial infarction) or a stroke.[2]

1.2 Chronic Total Occlusion

As plaque continues to develop in the walls of the artery, the vessel lumen narrows down. The reduced lumen is usually asymptomatic, until an acute problem is developed, downstream of the original constriction. The plaque development may continue within the weakened artery and result in complete blockage, with zero or little blood flow and the formation of a chronic total occlusion (CTO).[3] Chronic total occlusions are primarily found in coronary arteries, which is a common site for atherosclerotic plaque to develop. Coronary arteries are specific blood vessels that originate from the cusp of the aortic valve at the junction of the aorta and left ventricle. They provide oxygen rich blood to the cardiac muscle to keep up the pumping action of the heart and whose etymology is derived from the crown like fitting around the heart. These total occlusions may exist in the coronary arteries for greater than three months. [4] Flow within the arteries beyond the occlusion may be TIMI 0 (Thrombolysis in Myocardial Infarction) where antegrade flow may be absent or TIMI 1 a faint antegrade flow of blood.[5] It is not uncommon for multiple CTOs to be formed within the same individual which can result in angina (chest pain) or even a heart attack. It is suggested that around 19% of patients with coronary artery disease have one or more CTOs.[6]

1.3 Diagnosing and treating Chronic Total Occlusions

CTOs may remain asymptomatic for some time, after which the low flow of blood generally creates problems in the heart, developing symptoms that signal the presence of a CTO. Symptoms include chest pain or angina, fatigue, shortness of breath, nausea, irregular heart beat or rhythm, numbness and weakness.[7] CTOs are associated with a number of risk factors including family history of heart disease, diabetes, high cholesterol, hypertension, obesity, smoking and lack of exercise, many of which can be accommodated for with healthy life choices. Age, sex, and diet also play a significant role in causing atherosclerosis and development of CTOs.[3],[7] CTOs usually go undetected until manifestation of an associated heart disease like heart failure. Noninvasive

procedures like EKG, MRI or CT scans can be used to detect the presence of CTOs.[8],[9] Minimally invasive procedures like coronary angiogram can also identify CTOs present in blood vessels. In a coronary angiogram, a catheter is inserted in a peripheral artery, frequently the femoral artery, and driven towards the heart until it reaches the origin of the coronary arteries where it is navigated to the point of interest and a die is injected. Subsequently X-ray imaging is performed to observe the absence or presence of the dye downstream of the point of injection where a blockage is suspected. The location and size of the coronary artery generally plays a significant role in determining the difficulty of the diagnosis of CTOs. The size of available catheter limits the locations that can be visualized and novel techniques that incorporate smaller and more flexible scopes are being developed to reduce the cost and risk associated with these different diagnostic techniques, such as removing the need for suturing post catheterization for some catheters.[10] New and improved technologies are establishing platforms for biomedical imaging and clinical diagnosis at a remarkable rate.[11]

It has been proven that treatment of CTOs has improved the quantity and quality of life, while also enhancing the functioning of the heart and reducing symptoms like angina.[12],[13] Treatment of CTOs is done using different methods such as angioplasty, percutaneous coronary intervention, coronary artery bypass surgery, or even atherectomy which involves breakdown of the plaque.[12] Clearing of blockage using interventional techniques is relatively intrusive in comparison to creating a detour in the blood vessels using a coronary artery bypass surgery. In an angioplasty or a percutaneous coronary intervention (PCI) a catheter is inserted into the body, driven all the way up to the blockage where a stent is deployed. The stent expands inside the artery pushing the plaque towards the distal region of the lumen, hence opening up the artery for the flow of blood.[14],[15] A significant amount of patients with a CTO choose to undergo PCI, with its high success rates

associated and a favorable risk/benefit ratio.[16] In patients where PCI failed to clear the CTO, laser atherectomy can be used to re-canalize the artery. Laser atherectomy is considered the final method to treat undilatable lesions in coronary arteries.[17] Laser catheters employed in this treatment help soften or loosen the plaque and prepare for subsequent angioplasty if required.[18],[19] Catheter-based treatments of CTOs is considered as the final frontier in interventional cardiology.[20]

1.4 Angioscopy using catheters

Catheters are a medical device consisting of a thin tube composed of different medical grade materials, to be inserted into body cavities, vessels or ducts. Catheters serve a wide range of functionalities but are primarily used for administering fluids or gases, assist in drainage of fluids, or provide access to diagnose organs located in hard to reach regions. Catheters are usually tailored in design to meet their functional requirements which can vary such as urological, cardiovascular, gastrointestinal, and neurovascular applications. Cardiologists make use of catheters for coronary angiograms and other contrast injection techniques. In addition, interventional cardiologists use them for treating different cardiovascular diseases like aneurysms and CTOs by gently steering guide wires and catheters toward the site of the disease. Typically, cardiac catheterization takes place by entering the body either via the radial artery in the arm or the femoral artery or vein in the leg. As technological advancements continue, catheter design continues to grow more complex and intricate with smaller sizes available that are now able to reach narrow vessels like the coronary arteries located on the heart.

Catheters are manufactured in a large variety of designs. Some have a flexible tube that is driven using a guidewire which helps provide the path for which the catheter can follow to reach the desired location. Catheters consist of one or more channels through which substances can be either administered to, or withdrawn from, the region of operation. Some catheters are equipped with an

inflatable balloon that restricts the lumen they are in to stop the entry of substances, e.g. blood, for the course of the procedure. Catheters may or may not have optical channels through which the lumen they are in can be illuminated and imaged, with the objective of either treat a condition or simply optical diagnosis. Specialized catheter tool tips also exist that have auxiliary instruments and attachments required for the various procedures which are specific to different medical operations.

1.5 Saline Flushing

In an endovascular endoscopic procedure, the catheter is inserted into one of the major blood vessel connected to the site of operation and driven to the desired location usually with the help of a guidewire. Once at the proximal location of the cardiovascular disease, operation or treatment can take place. In the case of a CTO, this region is the proximal part of the atherosclerotic plaque. However, in comparison to gastrointestinal endoscopic operations, the lumen of blood vessel is opaque due to the presence of erythrocytes or red blood cells that do not allow for light to propagate through the blood lumen. This complicates optical diagnosis and treatment of the condition. In such cases, saline is injected via one of the lumens present in the catheter to clear or push the blood away, e.g. “saline flushing”. Saline flushing fills the catheter lumen with saline, which can be used to push contrast medium and other medication to the site of the catheter. Saline is known to help in scanning of sections of the body by reducing the artifacts that arise during visual analysis. In laser atherectomy, saline flushing helps reduce the temperature rise from the heat generated by the laser, keeping temperatures within the artery close to physiological levels.[21] Incomplete clearance of blood restricts imaging and diagnosis of CTOs, which mainly arises due to varying parametric and geometric conditions of the blood vessels.[18][22] Previous studies have provided suggestions on how to improve saline flushing to obtain better quality images in endoscopic procedures, but

damage to vessel walls has been observed in occlusion-infusion catheters.[18] These complications that arise during the treatment of CTOs beckons the need for understanding of saline flushing mechanics within arteries.

1.6 Improvements in angioscopes

Over the past few years, technological advancements in the fields of biomaterials, optics, instrumentation and control, have led to improvements in catheters. An intravascular catheter system was developed in and patented in 2000, in which occlusions are treated using opening members that are actuated using external plungers. It contained plural optical fibers and a rotating imaging shaft. The optical ends of the catheter are designed to close when flushing takes place using a suitable fluid.[22] Another catheter procedure was developed involving a pulsed laser beam to thermally degrade the atherosclerotic plaque or occlusion within the artery. A balloon is used to occlude the artery and prevent entry of blood from the heart, with saline used as a medium to fill the balloon. The catheter consists of a single optical channel which is primarily used for the laser.[23] Previously, a catheter was developed specifically for angio-surgery. The key feature of this device, invented by a team at the Massachusetts Institute of Technology, was the presence of an optical shield at the distal end of the catheter. The shield is mainly used to ‘displace’ the blood proximal to the atherosclerotic disease, in addition to protecting the catheter and fiber optics from intravascular substances. This also helps in avoiding any accidental damage to the patient vessel from the catheter tip. The optic shield maintains contact with the plaque tissue while a laser is used to degrade it. The parameters of the laser are optimized using an auxiliary computer.[24] Using similar technology, catheters with spherical lenses were developed. The spherical lens helps focus the laser onto a small concentrated region to interact with the plaque. With the help of an end cap on the catheter tip, residual energy from the laser is dispersed, which increase the rate at which the

plaque is burnt away. The catheter is also equipped with electrodes for ablation of electrical conducting tissue in heart treatment operations. Here, sapphire and silica are utilized in the lens for clearing of the plaque.[25] A different catheter design incorporated the use of a similar semicircular shield. It also contained a converging nozzle for the irrigation or flushing mechanism to increase the velocity of the flushing jet. This design, however, did not have an optical lens for imaging the plaque during treatment.[26] Another system was developed that used techniques involving different catheters. Initially, a laser is used to create a drilled core within the plaque. The drilled core provides room for a flexible element to attach itself onto the plaque. The plaque is then removed pulling on this flexible element attached to the drilled core, and the artery is cleared with the retraction of catheter.[27]

1.7 Motivation for current research

A team at the Human Photonics Lab at the University of Washington, has been working on developing imaging techniques used in endovascular catheters.[8][10][11] The cutting edge technology developed at this research lab is creating new avenues in terms of optical imaging and sensing of disease inside different lumens in the human body. Recently, a scanning fiber endoscope with a size of 1 mm housing a full-color imaging wide-field lens was designed by the team. Their innovation produced remarkable results and can be integrated into different diagnostic modalities.[11] However, the improvements in this direction account primarily for technical advancements in the imaging. By introducing improvements in the dynamics of blood and fluid interactions influencing the flow of blood revolving around the area of interest, further technological advancements in these catheters can take place in parallel.

A new physics-driven approach to designing catheters provides a platform to understand the fluid mechanics involved. By exploring the saline-blood interaction, catheter design can be optimized

to maximize the space requirements on the catheter cross section. Pressure analysis within the entire flushing system is crucial and is has not been investigated in detail previously. In an already weakened artery, the development of overpressure due to injection of a new fluid is a risk in the diagnostic or surgical operation. Rupture of the artery can take place in an attempt to treat it, exacerbating the risk factor and increasing the complications associated with the technique. Hence, to help improve the methodology involved in the developing upgraded catheters as well as to minimize any uncertainties in the entire process, it was proposed to use CFD as a tool to investigate and provide recommendations on catheter development.

Chapter 2
METHODOLOGY

The objective of this thesis is to use computational simulations to understand the fluid dynamics during saline flushing in the treatment of chronic total occlusions. In this chapter, the methods used to achieve the aforementioned objectives are described in detail. Computational Fluid Dynamics (CFD) was utilized to simulate the blood pressure, fluid flow and the mixing of saline and blood that occurs when saline is injected into the arteries. By starting from basic catheters with minimal complexity, the necessity of new functionality was met by introduction of different features that increased the intricacy of the catheter and the novel catheter control technique proposed towards the end of the study. Finally, a new method to accurately estimate when treatment and visual analysis of the CTO is possible through the catheter is discussed, which can supplement the computational analysis in this thesis.

2.1 Domain Geometry

For the study, the region of interest consisted of the distal end of the catheter that was located at a short distance in front of the CTO. The CTO is present inside a small section of the coronary artery. The catheter designs were continuously modified with changes to other parameters involved in the saline flushing. All the required geometries for the catheter models were created using the in-built CAD modeler in StarCCM++ (CD-Adapco/Siemens, Melville, NY). Three different catheter designs were modeled: 1.) a co-axial annulus function as a saline injection channel, 2.)

diametrically opposed saline injection and suction channels and, 3.) adjacent saline suction and injection channels. The design changes for the catheters were dictated by the CFD results that required new improvements to enable better flushing of saline. In simulation models where the total pressure drop was to be predicted along the entire length of the catheter, an equivalent pressure drop lumen was created to mimic pressure drop without having to simulate over a meter of catheter lumen. The design process for the catheters took an evolutionary approach. StarCCM++ was used to create all the additional elements in the geometric models. The computational domain essentially contains an artery with a CTO and a catheter within it. The base artery diameter is 2.7 mm, which is an approximate size for the left anterior descending (LAD) coronary artery where the CTOs are commonly found.[28] The catheter size to accommodate within this artery comfortably was selected to be 5 French units (Fr) or about 1.67 mm.[29] The stand-off distance, which represents the distance between the catheter tip and the CTO, was set to be equal to one diameter of the artery (1D=2.7 mm). This distance was fixed for all simulations involving an inflatable balloon occlusion as well as for simulations with the absence of a suction lumen within the catheter. The length of the catheter and artery simulated varied depending on the location of the outlet for the blood saline mixture. In most cases, this was a length of 5D or 13.5 mm. With the introduction of a suction lumen, the domain of simulation was reduced to 6.7 mm. In cases where equivalent pressure was to be predicted, the length of the catheter inserted into the body was selected to be about 1 meter. This incorporates the point where saline is pushed into the catheter, as well as the site of introduction into the vasculature, either the radial artery or femoral artery/vein. The equivalent pressure drop lumen is incorporated by creating an entry length tube using a smaller diameter, using the laminar scaling that determines linear dependency of pressure drop with length

and fifth power dependency of pressure drop with lumen diameter, to account for the pressure loss that occurs inside the catheter lumen before being injected into the artery.

The main function of the catheter for diagnosis or for treatment requires additional space on the tip of the catheter for auxiliary instruments. Hence, there is need to provide room for this accommodation within the catheter, by minimizing the lumen space for saline infusion which is a major design consideration.

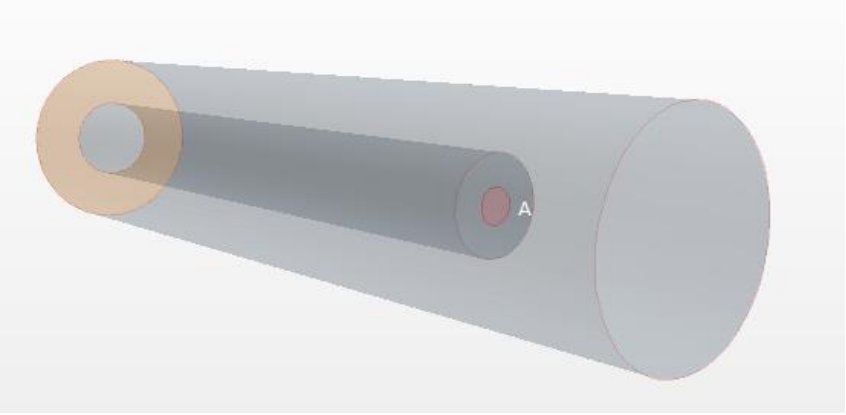

(a)

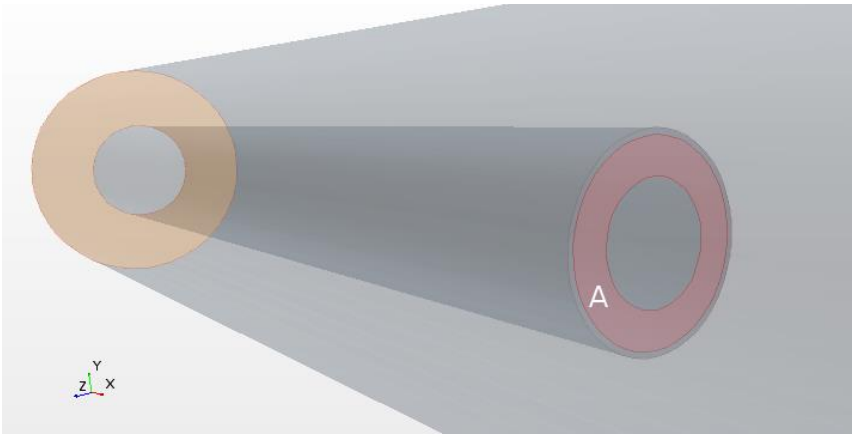

(b)

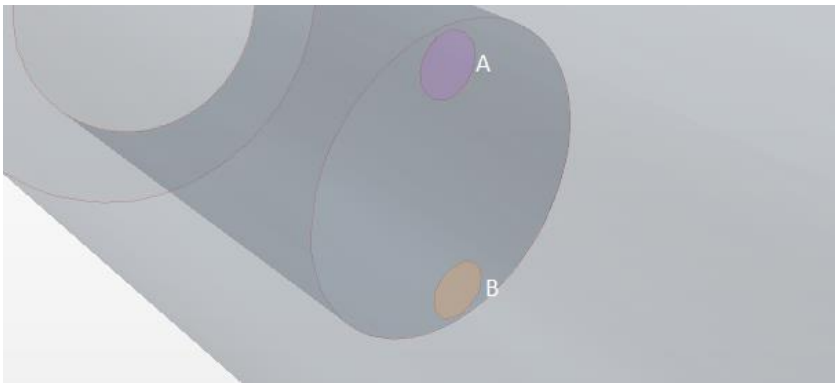

(c)

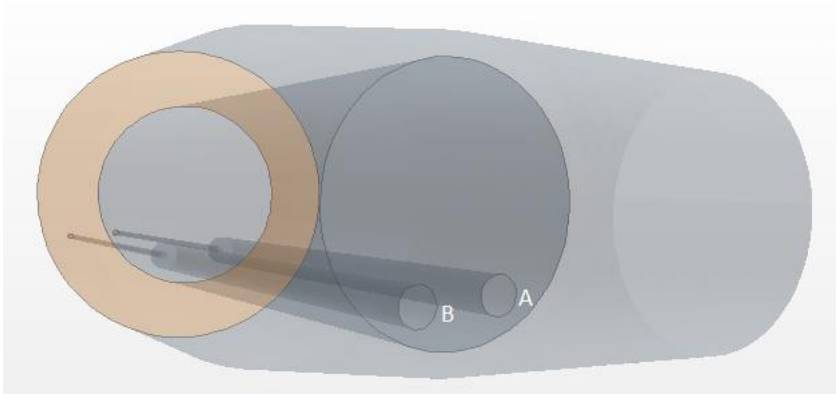

(d)

Figure 2.1 Different catheter design geometries: central injection (a), annulus injection (b), suction catheter (c), adjacent lumen catheter (injection/suction) (d). The region marked 'A' represents saline injection lumen, while 'B' marks the suction lumen.

2.2 Mesh Generation

The computational domain is spatially discretized as part of the procedure in solve the numerical equations. StarCCM++ is a finite-volume solver that divides the domain into specific control volumes (the finite volumes), as opposed to other numerical solvers which use finite differences or finite elements. A tetrahedral volume mesh is generated for the simulation domain which employs tetrahedral volumes throughout the entire domain. On the walls of the fluid domain (arterial and catheter walls, as described later), prism cell layers are developed to provide accurate

analysis near the boundaries of the flow. The selection of an unstructured grid reduces the time involved in generating the mesh while providing satisfactory simulation results. The global element size is set to 75 microns and 4 prismatic layers are used along the boundaries. The target size on the surfaces was set to 100%, while the minimum surface size was fixed at 10% of the global element size. The number of points set on a curve for a complete circle was maintained at 36. Through the entire domain, subsequent cells were allowed to grow at a rate of 1.3 and the stretching of prism layer was fixed at 1.5 times the original cell size. This was controlled with an overall prism layer thickness of 25 microns. As the number of cells in the mesh increase, the computational demands increase as well. A fine mesh helps provide more accurate results, but comes at a cost of longer simulation times. In CFD, a fine balance is required to be achieved between the accuracy of the solution and the computational costs associated with it. By selecting an excessively fine mesh, it is possible to obtain an insignificant gain in the solution accuracy. However, an unresolved mesh will result in inaccurate predictions of the solution. Hence, a grid validation study was done to obtain the optimum mesh qualities. The resulting number of cells in the simulation were between $8.0x10^5$ to $1.4x10^6$ cells depending on the length of the simulation domain.

2.3 Boundary Conditions

To simulate the flow in the domain, the physical conditions that take place within the artery are adopted in CFD simulations using boundary conditions and initial conditions. The boundary conditions mimic the underlying physical conditions which can then be used to drive the simulations. The simulation domain is defined by 4 different boundaries. An inlet, an outlet, an artery opening inlet, and wall boundary conditions. The wall boundary conditions essentially represent all surfaces through which the fluid in the simulation is unable to flow through. In our

case this is represented by the catheter walls, the arterial walls, as well as the impenetrable CTO. Saline is injected into the artery from the catheter which represents the flow inlet condition. The inlet condition in CFD is generally applied either in terms of pressure or velocity of the incoming fluid. The outlet boundary condition explains how different fluids within the system leave the domain or our control volume. For conservation of mass to take place, an equivalent mass equal to the fluid entering the system must exit instantaneously. This is possible via an outlet condition that physically represents either the distal end of the artery or a suction lumen in the catheter (or both), where a saline-blood mixture exits the region of interest. To simulate the flow of blood pumped by the heart, an additional pressure inlet boundary condition was used, where the fluid that would come into the domain would be blood instead of saline. The specific values of the boundary conditions are detailed below:

Inlet

At the inlet surface, a constant pressure condition is maintained in most simulation cases. The pressure applied is varied depending on the required simulation. In simulations where a constant velocity inlet condition was imposed, the pressure equivalent velocity values were determined, to enable similar simulation physics as in the pressure driven inlet conditions. The inlet fluid is selected as a pure saline solution and the flow direction is normal to the inlet surface.

Outlet

The outlet domain is defined as a pressure outlet. The pressure outlet initially was set as 0 Pa, which provides the gage level for the pressure within the rest of the simulation domain. The affinity or permeability of this surface to both blood and saline was set to be 1, which means that there is no preference to any of the two fluids within the simulation. In some simulations, a net negative

pressure was applied to investigate the effects of suction. Where a mass flow control was studied, the outlet was changed to velocity-specified outlet as opposed to a pressure outlet to observe the effects of coordinating the suction flow rate with the saline injection flow rate.

Artery Inlet

An additional inlet was created to simulate the ambient blood flowing from the heart into the coronary artery. This was used in simulations where the artery was kept open (not occluded with a balloon proximally) during the flushing as well in cases where the artery was not completely occluded using balloon inflation. Patient specific data was extracted from a previous study on the left anterior descending coronary artery. The patient blood pressure was then applied periodically at the proximal end of the occluded artery to introduce the cyclic effect of the blood pumped into the coronary artery.

Wall Boundary Condition

The arterial wall and the catheter body are simulated as rigid walls with a standard no-slip condition, $u = 0$ at the wall.

2.4 Simulation Physics

The simulations are setup as a multi-component liquid, where the two components are blood and saline. Each individual component is simulated with constant density. The conservation of mass and momentum equations are solved to obtain the velocity and pressure values throughout the domain:

$$\nabla . u = 0$$

$$\frac{\partial u}{\partial x} + u \,.\nabla u = \, -\nabla P + \mu \nabla^2 u$$

Using StarCCM++ 12.02.010 (CD-Adapco/Siemens, Melville, New York, USA), the incompressible Navier stokes equations are solved in three dimensions. The flow properties within the simulation are such that the flow remains laminar through the entire simulation. To advance the time step, a first order implicit time-stepping scheme is applied, which provides the required unsteady conditions for the simulations. The time step for each simulation is $1x10^{-5}$ seconds and the simulations run for about one second, or till clearance is achieved. Clearance in the simulations is considered when there exists 98% saline concentration by mass fraction between the tip of the catheter and the CTO. Saline is modeled as a liquid with physical properties similar to water, while blood is assumed to have a density of 1050 kg/m3 with a viscosity of 3.5 cP. The fluids are selected to be non-reactive in terms of their chemical properties.

Multi-component fluid mechanics

A multi-component mixture is a miscible mixture of two or more pure substances in the same phase. Each individual fluid is initially defined in terms of its density, viscosity, and molecular weight. Subsequently, the mixture properties are to be specified to predict how the two fluids will interact with each other. The mixture properties are defined as the combined density, dynamic viscosity, molecular diffusivity, and molecular weight.

Combined Density

The density of the mixture is calculated based on the volume-weighted mixture function. The function can be described as:

$$\theta_{mix} = \frac{1}{\sum_i^N (\frac{y_i}{\theta_i})}$$

where θ_{mix} is the density of the mixture, N=2 for our case, y and θ are the volume fraction and density of the specific component at that location respectively.

Combined Dynamic Viscosity

The dynamic viscosity of the mixture is calculated based on the mass-weighted mixture function. The function can be described as:

$$\emptyset_{mix} = \sum_{i=1}^{N} y_i \emptyset_i$$

where $\emptyset_{mix}$ is the dynamic viscosity of the mixture, N=2 for our case, y and $\emptyset$ are the mass fraction and dynamic viscosity of the specific component at that location respectively.

Molecular Diffusivity

The molecular diffusivity of the two fluids is defined in terms of the Schmidt number. The Schmidt number is a non-dimensional defined as the ration of momentum diffusivity and mass diffusivity. It characterizes fluid flows that have both mass and momentum diffusion convection processes. Ideally it denotes which of the two processes, i.e. the molecular or momentum diffusion, is predominant The Schmidt number is defined as:

$$Sc = \frac{\nu}{D} = \frac{\mu}{\rho D}$$

$$Sc = \frac{viscous\ diffusion\ rate}{molecular\ (mass)\ diffusion\ rate}$$

where *Sc* is the Schmidt Number, *v* is the kinematic viscosity, *D* is the mass diffusivity, μ is the dynamic viscosity of the fluid, and ρ is the density of the fluid.

For the simulations presented here, the Schmidt Number was set to 1. A Schmidt number of unity signifies that the molecular diffusion process is comparable to the momentum diffusion process. However, in the physics concerning the problem of catheter imaging and optical clarity of the fluid between the catheter tip and CTO, the molecular diffusion process is negligible. By establishing the Schmidt number to unity, our simulations grossly overestimate the molecular diffusion process, which will have a minor influence in the actual physics studied. This helps to make the simulation time manageable even if it ignores the mixing of saline and blood at the cellular or molecular levels, which will not affect the optical transparency.

The initial conditions prescribed within the simulation are realistic arterial conditions. The fluid within the entire domain is blood. The average blood pressure is set to 70 mmHg.

2.5 Simulation Parameters of Interest

Mass Fraction of Saline

Mass fraction of saline is the ratio of the amount of saline that exists at a particular location by mass over the total mass of the combined fluid (Blood and saline). It gives us an understanding of the transparency of the blood-saline mixture in front of the CTO, which is required to image the CTO. The required mass fraction to obtain clearance using saline flushing is 98% between the catheter and the CTO.

$$Mf_i = \frac{m_i}{m_{total}}$$

where Mf_i is the mass fraction of species *i*, m_i is the total mass of species *i*, and m_{total} is the total mass of all the species in the mixture.

Clearance Time

The time required to completely flush the blood using saline is a key parameter that is used to understand the saline flushing mechanism. The flow rate of saline into the artery is regulated to obtain the clearance within optimum time levels. It is primarily defined as, approximately, when the blood-saline mixture reaches an average mass fraction of 98% in the volume between the catheter tip and the CTO.

Reynolds Number

Reynolds Number is a non-dimensional number that helps characterize the fluid flow. It broadly serves to describe flow as either laminar or turbulent. Laminar flow has smooth streamlines and is represented by low values of Reynolds number while higher values of Reynolds number describe a complex and non-parallel turbulent flow. The Reynolds Number is designated as

$$Re = \frac{\rho V d}{\mu}$$

where Re is the Reynolds Number, ρ is the density of the fluid, V is the velocity of the fluid, d is the characteristic length , μ is the viscosity of the fluid, and ν is the dynamic viscosity of the fluid.

2.6 Optical Ray Tracing

Once the saline solution begins to push the blood away from the CTO, the transparency of the saline-blood mixture in front of the CTO increases. As light transmittance increases, the CTO can be imaged by the clinician for treatment. To understand the light propagation involved in the procedure, an optical ray tracing study was conducted.

Cone of View

The optical analysis assumed that the center of the catheter houses two optical fibers adjacent to one another. The optical fibers transmit light from a light source to the arterial cavity and return reflected light from the cavity to a sensor/monitor in the treatment room. This way, the region under visual inspection is a cone of view with the center of the catheter acting as a vertex and the base of the cone represented by the CTO. The fluid residing within this cone of view influences the visibility of the CTO while the adjacent mixture has negligible effect on the technique.

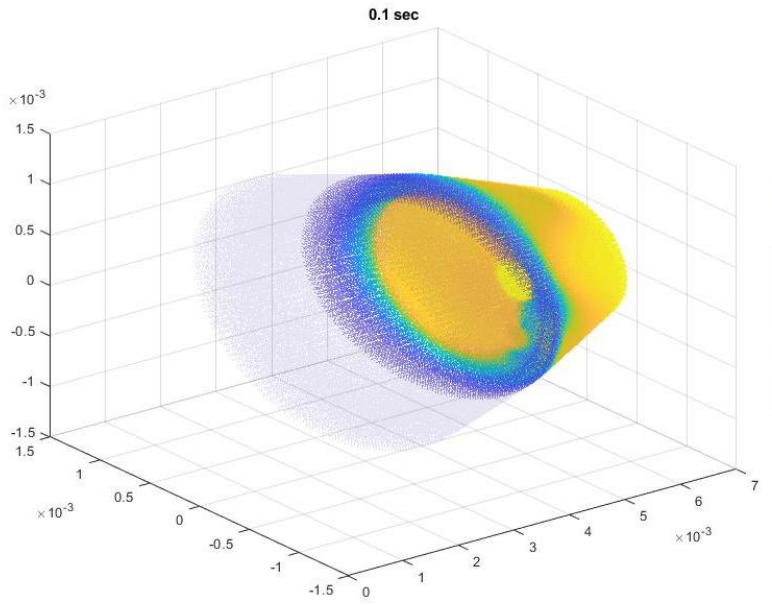

(a)

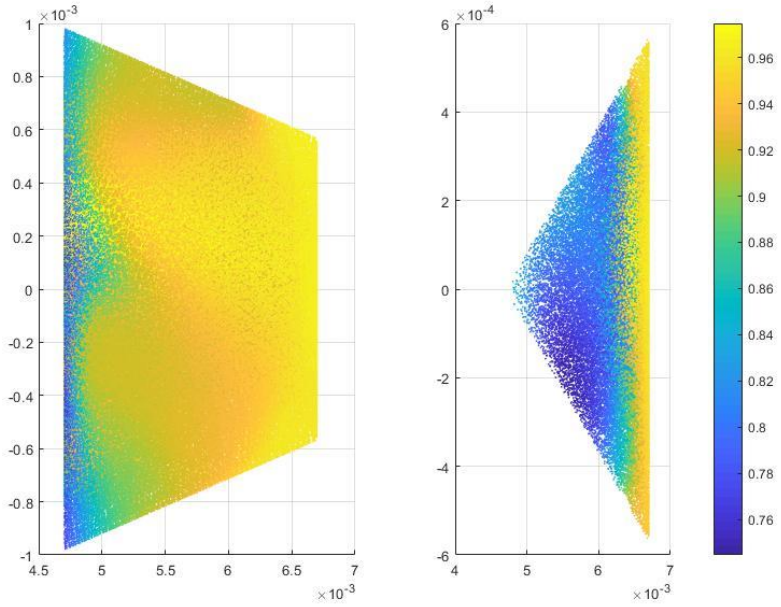

(b)

Figure 2.2 Developing the cone of view. The saline mass fraction data is extracted into Matlab (a). The region behind the face of the catheter is removed (b) (left) and then trimmed to the cone of view with the center of the cone at the catheter and the edge defined by the edges of the CTO (b) (right). The color bar represents

The mass fraction of saline from each simulation was sampled and extracted at every 0.01 seconds. The sampled data was introduced into MATLAB (MathWorks Inc., Natick, Massachusetts, United States) where the data is trimmed to represent the cone of view. The height of the cone is equal to the standoff distance between the catheter and the CTO. This standoff distance varied based on the plaque morphology of the simulation and was equal to 0.128 mm, 0.2 mm, 0.37 mm for zero clearance, steep wedge and shallow wedges respectively.

Optical Map

An optical map was generated based on interpolation of data derived from a study conducted earlier. The wavelength of light selected for the optical analysis was 505 nm. The optical map

generated provided the optical density of the blood mixture depending on the optical distance of through which the light would travel as well as the hematocrit concentration of the blood. About 408 light rays were projected from the center of the catheter to the CTO and the endpoints of these rays were uniformly distributed on the CTO surface. Each ray was broken down to a distance of about 0.0379 mm which represented an individual segment. The mass fraction of saline was used to determine the hematocrit of the blood present in each individual segment using the formula

$$HC = \frac{(1 - Mf_s) * 45 * 0.6206}{3}$$

where HC is the hematocrit of the segment, Mf_s is the mass fraction of saline, the original hematocrit of pure blood in the patient is set to be 45%, the divisional factor of 3 is used to convert the hemoglobin number to hematocrit. The factor 0.6206 is used to incorporate the unit conversion from g/dL to mmol/L when dealing with the hematocrit number.

The optical density was then calculated individually based on the hematocrit and the segment distance from the optical map developed earlier. The optical transmittance of each segment was then summed over the entire travel length and doubled to incorporate the reflectance of light from the CTO. This optical transmittance was using the equation

$$Tm = \frac{10^{(2-OD)}}{100}$$

where Tm is the Transmittance of light, and OD is the optical density or absorbance of light by the saline blood mixture.

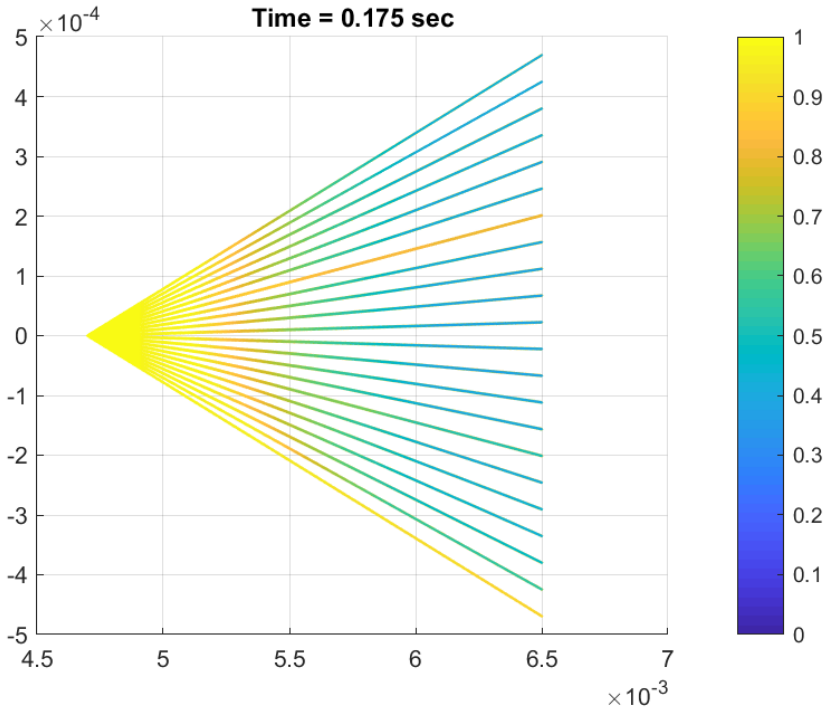
Time = 0.175 sec
×10^-4
5
4
3
2
1
0
-1
-2
-3
-4
-5
4.5
5
5.5
6
6.5
7
×10^-3
1
0.9
0.8
0.7
0.6
0.5
0.4
0.3
0.2
0.1
0

(a)

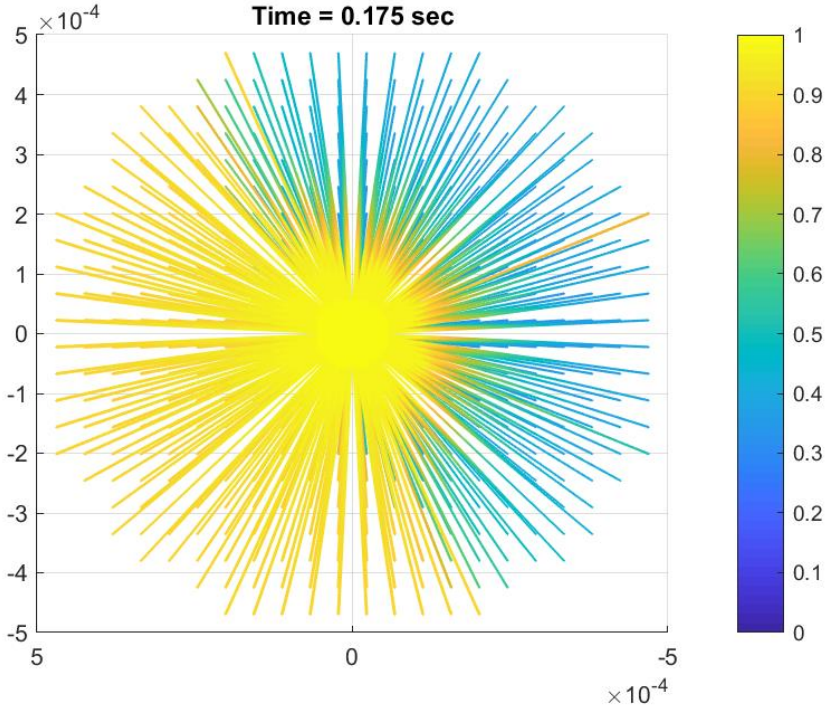
Time = 0.175 sec
×10^-4
5
4
3
2
1
0
-1
-2
-3
-4
-5
5
0
-5
×10^-4
1
0.9
0.8
0.7
0.6
0.5
0.4
0.3
0.2
0.1
0

(b)

Figure 2.3 Ray tracing from the center to the CTO using the optical transmittance. The side view (a) and the front view (b) of the ray tracing is shown. The color bar denotes the intensity of light that returns to the sensor after being reflected of the blood or the CTO.

Target Analysis

A checkered blue and white target was created that represented the visualization of the CTO. As the opacity of the mixture increased, the target is better visualized and the adjacent colors of blue and white are distinguishable from one another. A transparency level of 80% was selected as the threshold above which the CTO could be visualized. By comparing different images of the target, comparisons were made on the feasibility of the flushing technique and the characteristics of the catheter visualization technique were defined. When adjacent squares are clearly distinguishable as blue and white, the flushing or clearance is considered to be achieved.

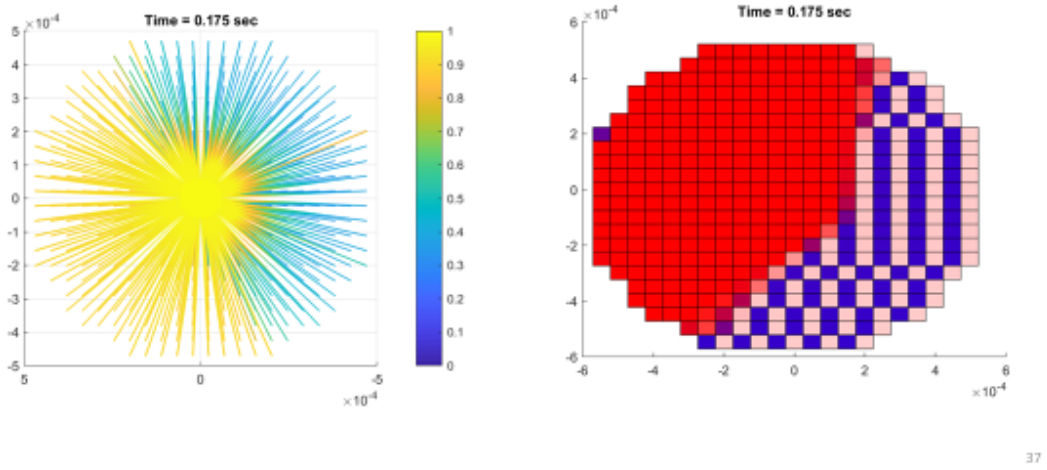

(a)

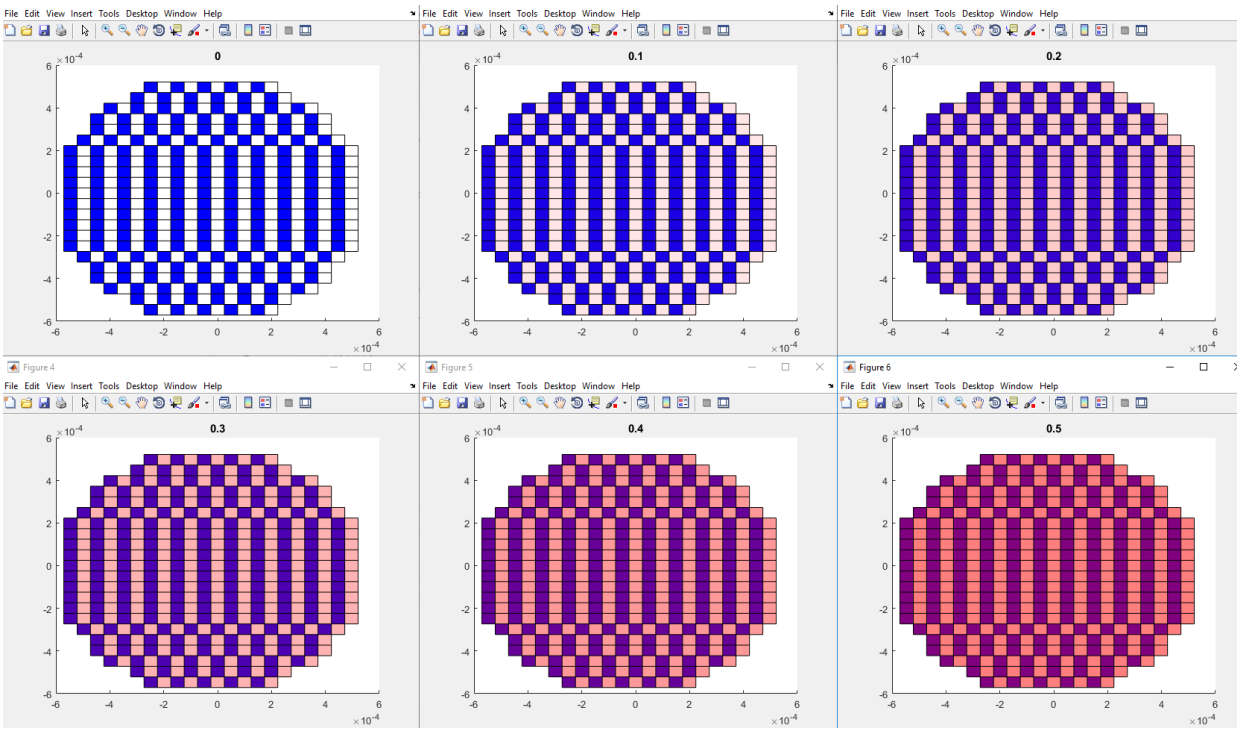

(b)

Figure 2.4 Target visualization to determine clearance of blood. The rays from the optical analysis are mapped onto the target to understand the region where blood interferes with the diagnosis (a) The red region represents the undiluted blood which prevents the viewing of the CTO. The right image is a mirror image of the ray tracing on the left. In (b) the different levels of clearance are displaced. The clearance threshold was selected to be 0.2 or (80% intensity of light) determined by comparing different levels of clearance where the red hue due to the blood is minimal.

Chapter 3
CFD SIMULATION FOR CATHETER OPTIMIZATION

The computational simulations provide information on the physics of saline flushing of blood, as a pre-cursor to visualizing or treating CTOs. By understanding the science behind this technique, it is possible to introduce changes in the catheter design which can be further studied using CFD. The work presented in the thesis is a novel approach to developing flushing catheters dictated by the fluid mechanics to improve visibility of the CTO to the interventionists. The design of the catheter took an evolutionary process as improvements were continuously added to enhance the flushing technique. Some of the designs showed promise hydro-dynamically but were later rejected for being associated with practical limitations.

3.1 Central Injection

The first catheter employed in the simulations consisted of a simple design. The model included a long straight artery, with a catheter housing a circular lumen coaxial with the catheter. The region of the catheter available for optical instruments was maximized by restricting the lumen diameter to 0.3 mm. The catheter tip needs to house different auxiliary instruments for diagnosis and treatment of the CTO, using the space provided in the region surrounding the circular lumen. The saline inlet mass flow rate was 2.0 cc/sec. The saline mixes with the blood in the arterial lumen and the resulting mixture exits the simulation domain at the proximal end of the artery. The arterial opening was not blocked using an inflatable balloon and, hence, remained unobstructed to fluid

flow. The proximal artery was also devoid of any pressure from the arterial blood pumped by the heart.

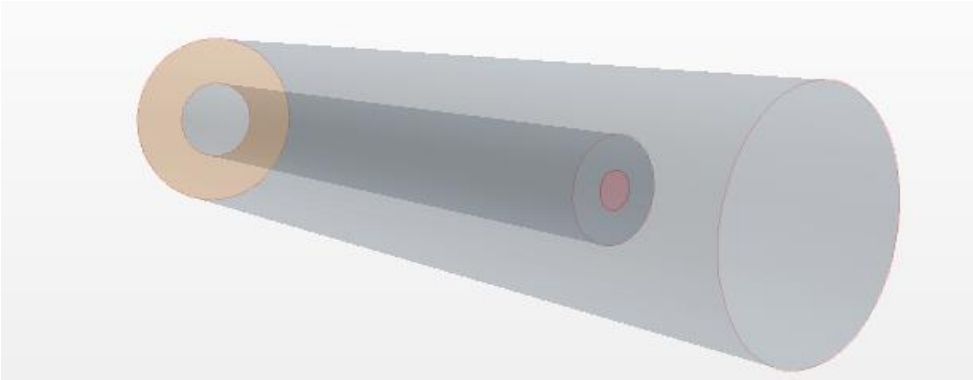

(a)

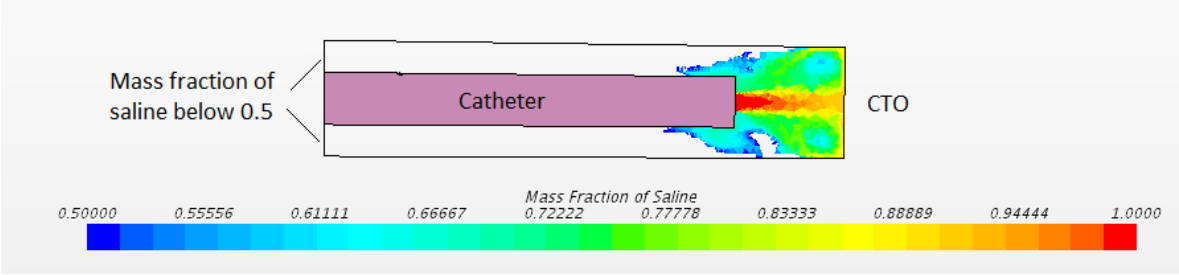

(b)

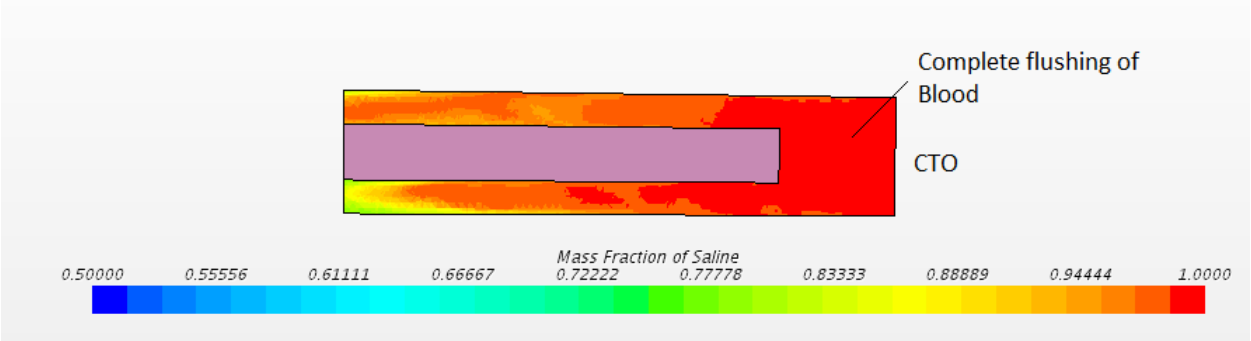

(c)

Figure 3.1 Central Injection Saline (a) showing a central saline injection geometry. The orange section denotes the outlet through which the saline-blood mixture exits the domain, while the inlet is

highlighted in red. (b) the fluid flow pattern injected at 2 cc/sec and (c) complete flushing of saline ahead of the CTO. All saline-fluid mixture with a mass fraction concentration of saline below 0.5 is clipped and is unseen in the simulations.

The resulting jet velocity of saline was 7.07 m/s and immediately flushed the blood as shown in Table 3.1. The saline jet as in Figure 3.1b) hits the CTO before spreading into the surrounding region. This jet then pushes the remaining blood to the proximal section of the artery while the remaining portion of the blood gets diluted in front of the catheter. The short flushing time of less than 0.1 sec was associated with a relatively high Reynolds number of 4700. The calculated pressure required to obtain such flow characteristics was about 3127 mmHg which is 32 times the average pressure within a coronary artery. In terms of saline flushing, the flushing was unnecessarily fast and the pressure developed was unsafe. This catheter was deemed to be overdesigned for the required functionality. By simplifying this catheter, a better design catheter can be employed while maintaining enough room for the versatility of the required catheter.

Diameter	Velocity	Time for flushing	Reynolds No.	Pressure (calculated)
0.6 mm	7.07 m/s	0.098 sec	4776	417 kPa

Table 3.1 Simulation results for a central injection system

3.2 Annulus Injection

To reduce the velocity of the saline jet, the area of injection was increased. This was done by incorporating a coaxial annulus as the shape of the lumen for saline injection in comparison to the previous standard circular lumen. The width of the lumen was kept the same as the diameter of the original central injection, hence maximizing the area available for additional utilities. The

available lumen area increased by a factor of 10, by placing it toward the outer edge and hence concentrating the instruments inside the center of catheter tip, as seen in Figure 3.2.

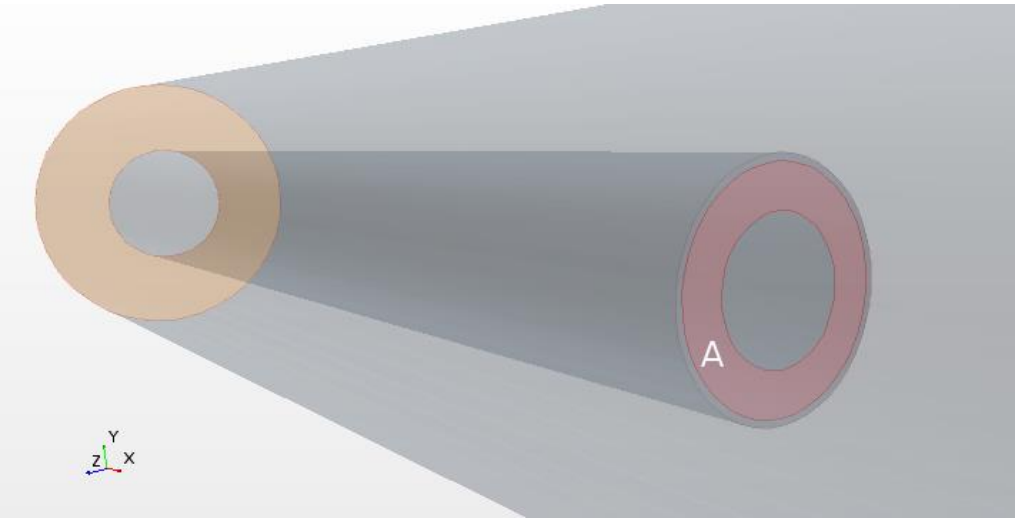

Figure 3.2 Annulus injection catheter. The annulus injection for saline is the region denoted by A. By pushing the injection to the outer edge, the space available in the center is used for optical and specialized instruments. The orange region represent the outflow of blood and saline from the simulation domain.

Varied mass flow rates

The annulus design was tested for three different flow rates of 1.00 cc/sec, 1.76 cc/sec, 2.00 cc/sec. The saline flows were varied by changing the inlet pressure of saline injection to understand the optimum flow rate which can bring about clearance quickly.

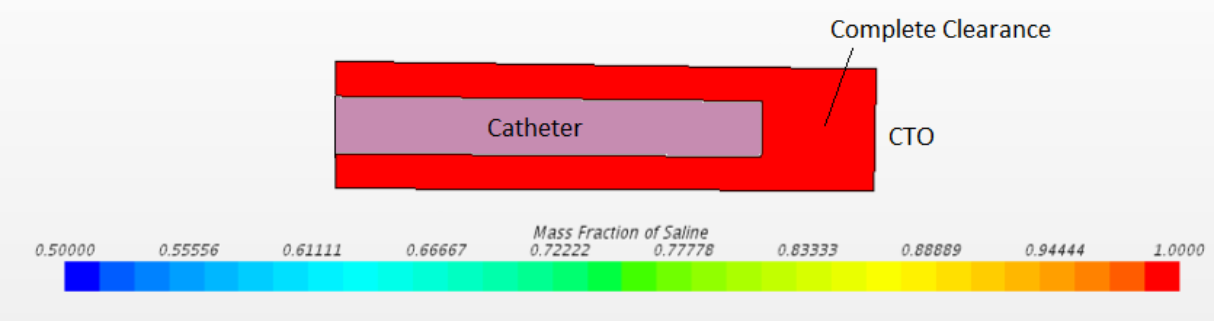

(a)

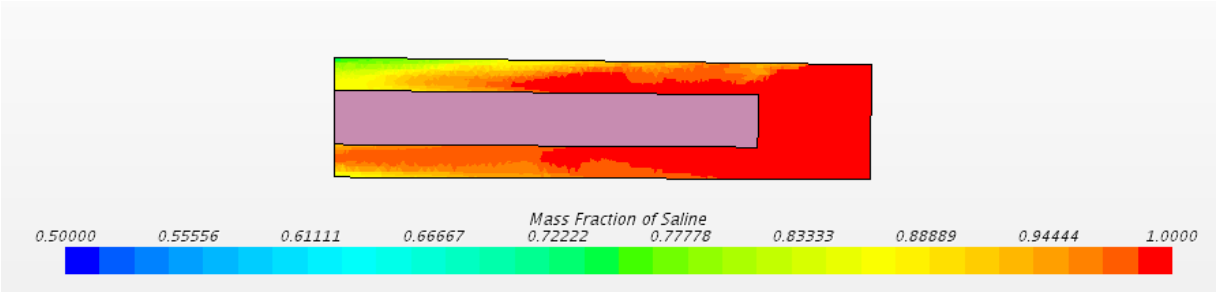

(b)

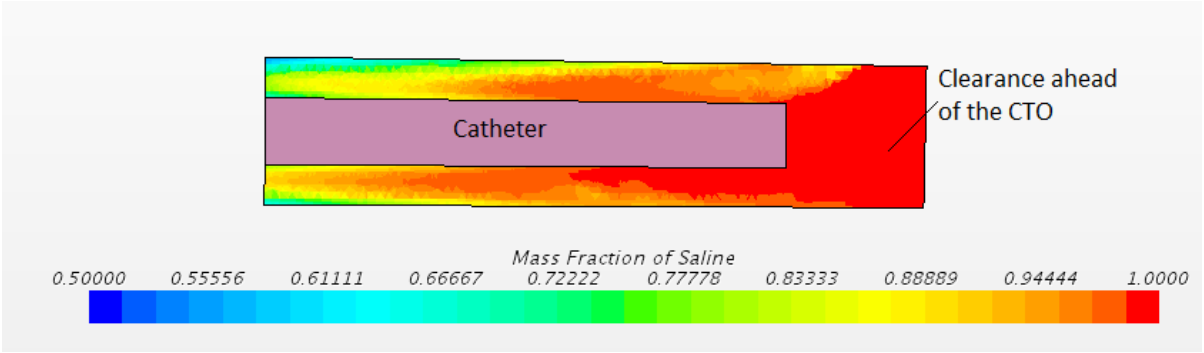

(c)

Figure 3.3 Clearance of blood using annulus injection catheter. Clearance is achieved in all three different mass flow rates of (a) 1 cc/sec (b) 1.76 cc/sec and (c) 2 cc/sec of saline into the artery. Clearance is required only in the region between the CTO and the face of the catheter.

Flow rate	Velocity	Reynolds No	Time for flushing	Pressure Drop (Calculated)
1.00 cc/sec	0.836 m/s	1433	0.812 sec	2292.97 Pa
1.76 cc/sec	1.470 m/s	2148	0.112 sec	5150.90 Pa
2.00 cc/sec	1.672 m/s	2867	0.084 sec	9171.86 Pa

Table 3.2 The influence of changing the mass flow rate of saline injection on the flushing mechanics in the catheter.

The Reynolds number in these cases dropped from turbulent values to transitional or purely laminar of about 1500 to 3000. As seen in Figure 3.3, clearance is achievable relatively easily for all three different mass flow rates. While the time to flush the saline increased, it remained well within an acceptable range of less than 1 second. However, the resulting pressure developed dropped drastically down to a maximum of 10 kPa as shown in Table 3.2. The significant drop is associated to the fall in velocity, with an effect proportional to the squared of its value on the pressure. Between the different flow rates of saline, the pressure drop increased corresponding to the flow rate, and by doubling the flow rate, it the pressure drop changed by a factor of four. These results are in accordance with Poiseuille flow inside a circular pipe.

3.3 Suction Lumen

In small arteries, the flushing of blood takes place slowly for the annulus design. The design works successfully for comparable artery and catheter sizes but falls in terms of efficiency as the artery channel reduces. While saline flushing is the prime objective of this study, the actual application of the catheter is complex and requires saline flushing as a means to enable its functionality. The annulus lumen reduced the area available for additional elements by half. To provide more room for tools available in the catheter as well as to mitigate the disadvantages of using the catheter in small arteries, a new design for the catheter was proposed.

In small arteries, the flushing of blood takes place slowly for the annulus design. The design works successfully for comparable artery and catheter sizes but falls in terms of efficiency as the artery diameter is reduced. While saline flushing is the prime objective of this study, the actual application of the catheter is complex and requires saline flushing as a means to enable its functionality. The annulus lumen reduced the area available for additional instruments by half. To provide more room for tools available in the catheter as well as to mitigate the disadvantages of using the catheter in small arteries, a new design for the catheter was proposed.

A suction lumen was introduced into the catheter, by which the blood-saline mixture can be sucked into the catheter, thus providing an exit to the fluid mixture proximal to the CTO. By pushing saline into the artery and removing the saline-blood mixture, an additional momentum component is introduced in the flushing mechanism. The annulus injection lumen is replaced with a circular channel for saline injection, and another additional channel of similar size is used for suction which is place diametrically opposite from the injection channel. With the outflow channel, the blood and saline can exit the region of interest quickly as opposed to moving around the catheter within the narrow clearance existing between the catheter and the arterial walls. Due to this, a relative vacuum is created between the tip of the catheter and the CTO, which is occupied immediately by the clear saline solution injected into the artery. This provides faster clearance and lower times of flushing. Additionally, the introduction of suction lowers the need for high mass flow rates of saline which in turn reduces the high pressure required to push the saline into the artery. The lower pressures developed inside the catheter are high enough to push saline but continue to remain within safe limits for the catheter design (around 100 kPa), which is near the nominal levels for injecting saline into the coronary artery. The pressure applied at the suction

lumen was maintained at atmospheric pressure, which provides the vacuum effect needed inside the artery.

3.4 Varying Lumen Diameters

The suction-based catheters were simulated with three different lumen sizes. The injection and saline channels were both modified simultaneously to be of 0.23 mm, 0.33 mm, and 0.43 mm seen in Figure 3.4. The results of the simulations are as shown in Table 3.3.

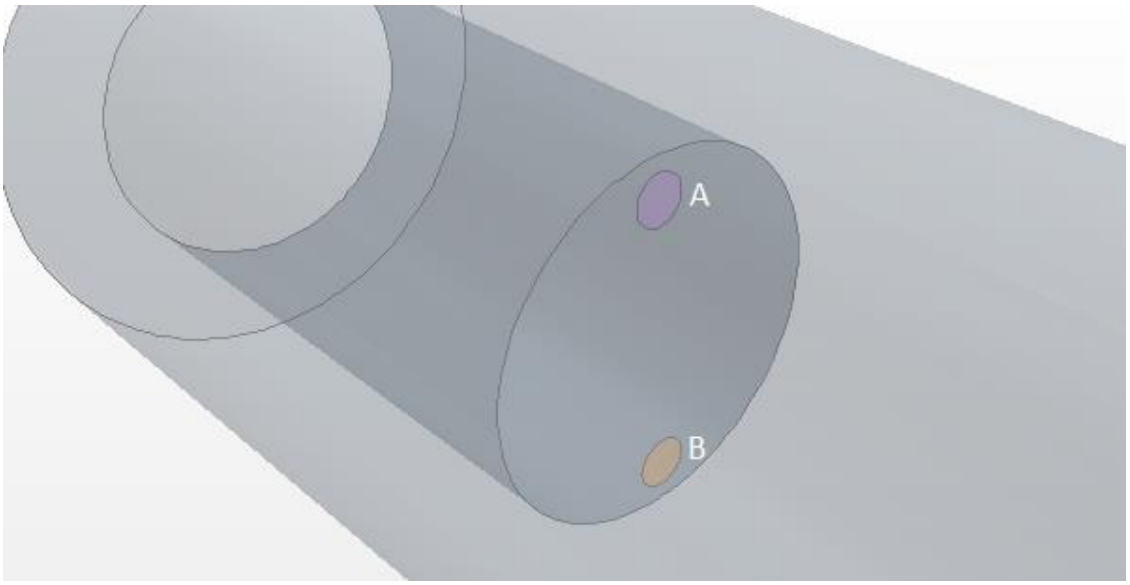

(a)

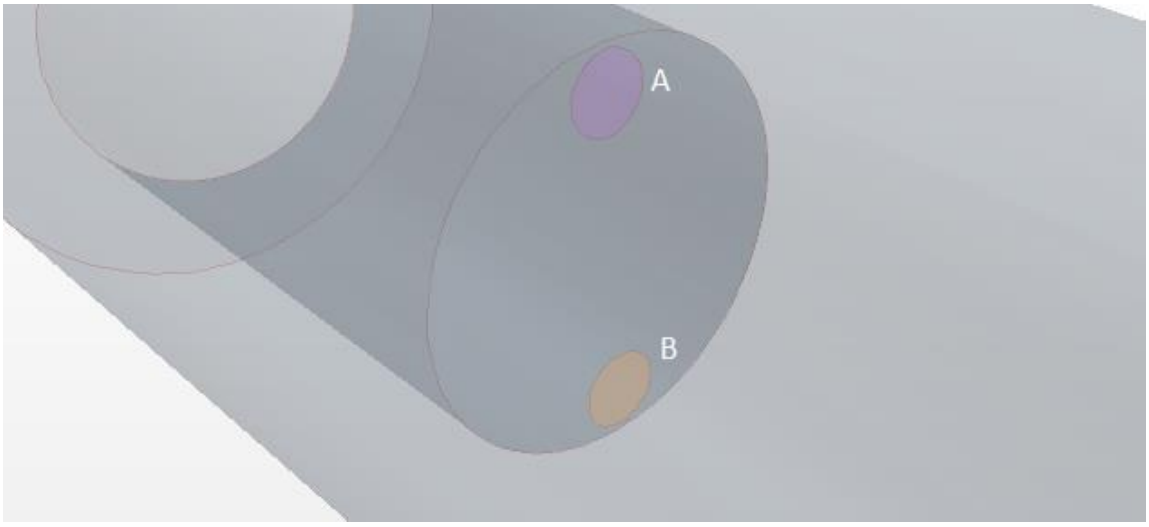

(b)

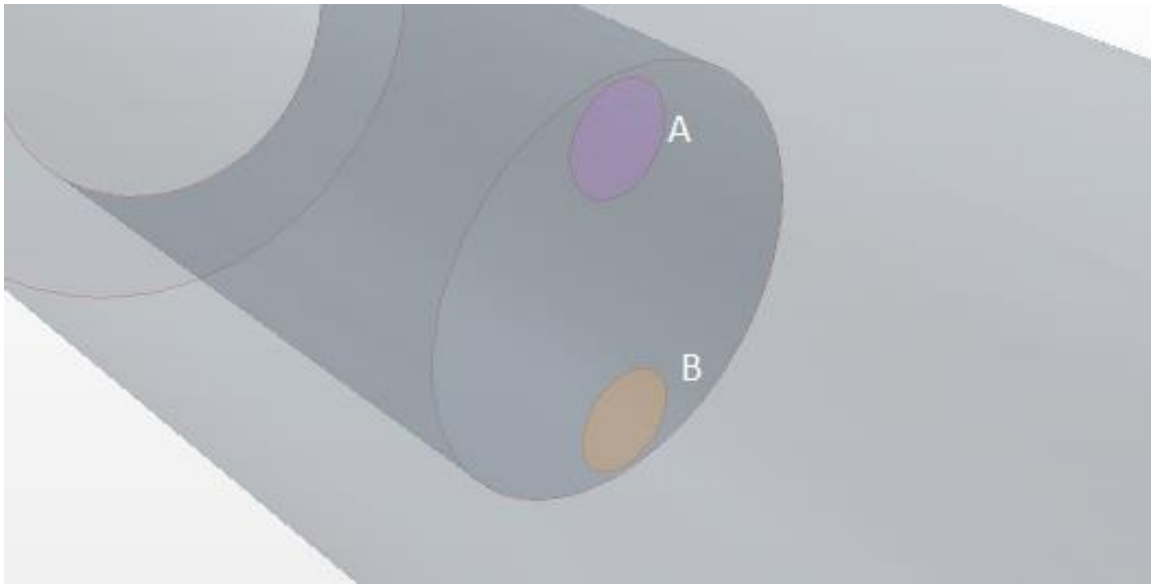

(c)

Figure 3.4 Comparing models of suction catheter. Geometric differences in the suction catheter design (a) 0.23 mm, (b) 0.33 m, and (c) 0.43 mm diameters. The change in the diameter of the lumen influences not only the fluid mechanics but also the space available for additional instrumentation. The purple regions marked in A inject saline into the artery and the orange regions marked in B suck the blood-saline mixture ahead of the CTO to create a vacuum.

Diameter of Inlet/Suction Lumen	Flow Rate	Velocity	Pressure Drop (calculated)	Time of flushing
0.23 mm	0.34 cc/sec	8.3212 m/s	1505.2 kPa	0.511 sec
0.33 mm	0.37 cc/sec	4.3477 m/s	286.0 kPa	0.530 sec
0.43 mm	0.35 cc/sec	2.4222 m/s	68.2 kPa	0.460 sec

Table 3.3 Influence on change in lumen diameter on the saline flushing dynamics

The reduction in the lumen diameters by 0.1 mm resulted in an increase in the velocity of injection by a factor of two. Consequently, the pressure drop required to facilitate such a fluid flow increased four times. This conforms to expectations in a Poiseuille flow in a tube. The desired effect of reduction in pressure is produced when the lumen diameter is increased, however this is associated with reduced space available for instruments and dissuades the pursuit of further enlarging of the lumen diameters.

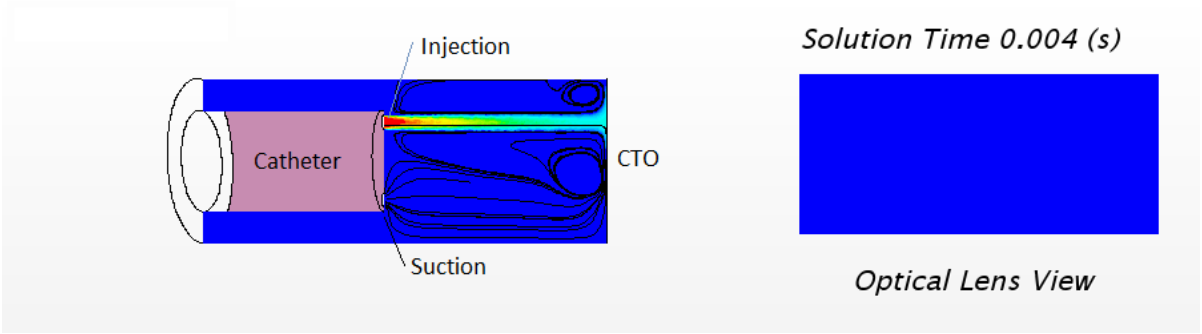

(a)

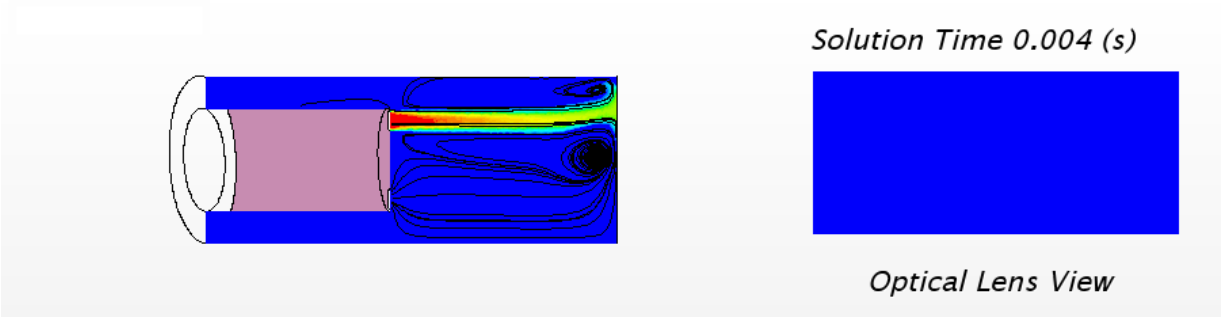

(b)

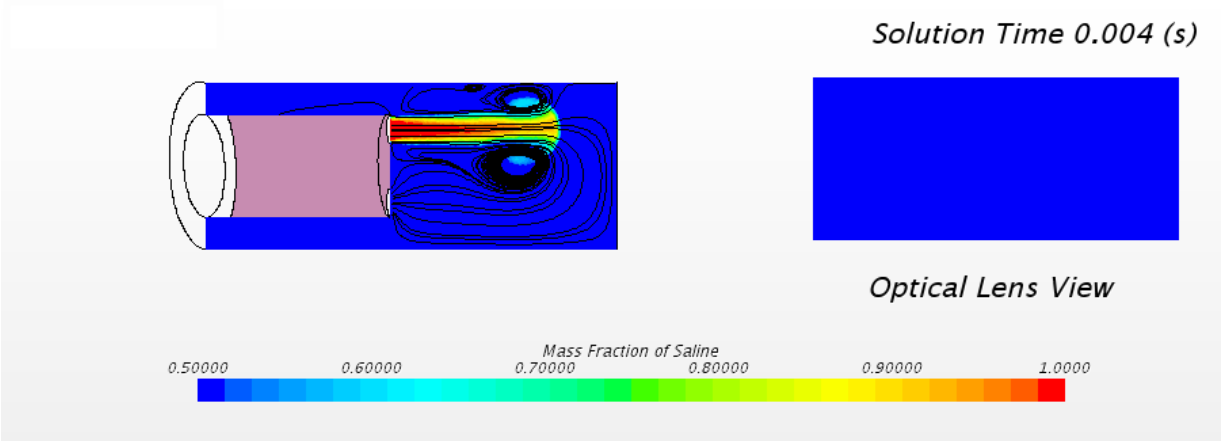

(c)

Figure 3.5 Saline injection pattern for different lumen diameters. As saline is injected, the three different lumens of diameters (a) 0.23 mm (b) 0.33 mm and (c) 0.43 mm create different flow patterns. The smaller lumens, create higher jet velocities that impinge the CTO as opposed to larger lumens. The optical lens view to the left shows blood occluding the vision of the CTO. The black lines represent the streamlines in the flow and show how the flow creates recirculating regions. Values <0.5 mass fraction of saline are displayed in blue.

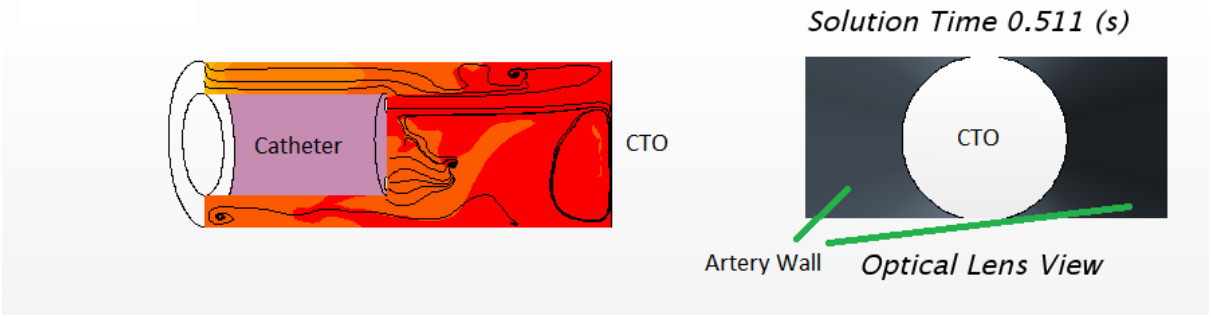

(a)

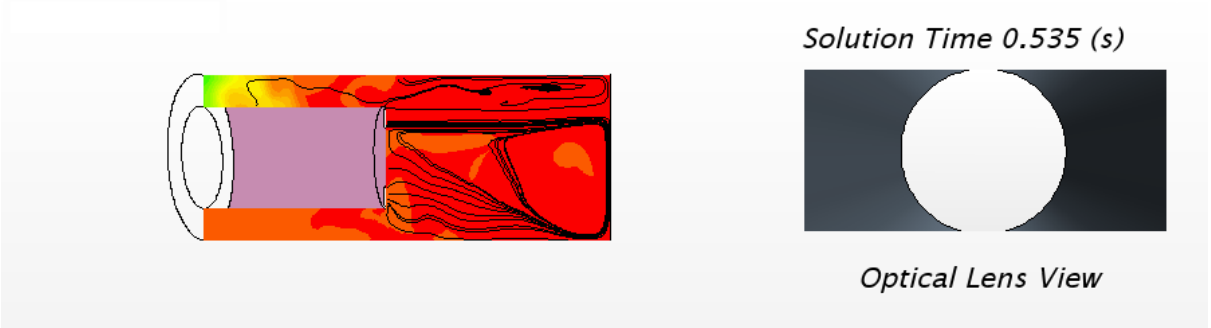

(b)

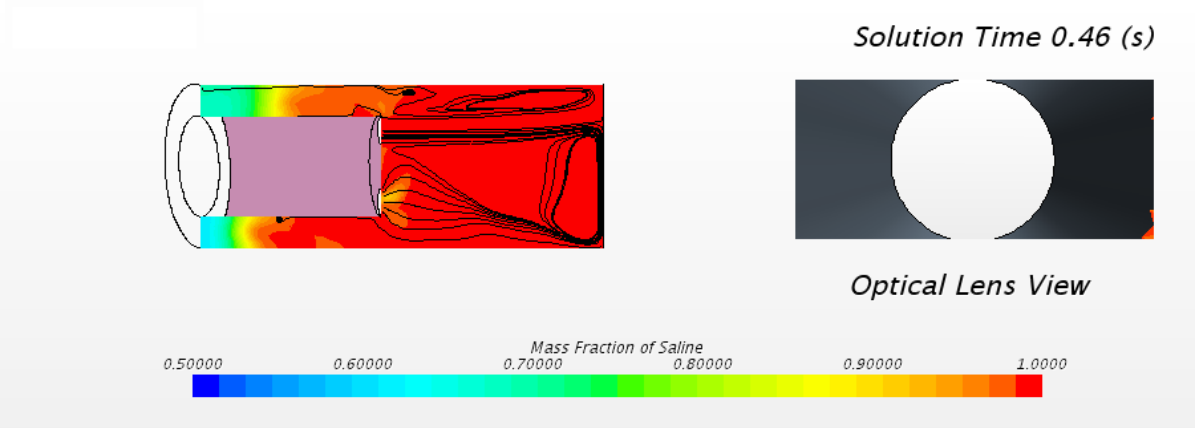

(c)

Figure 3.6 Clearance of blood using suction lumen catheter. Clearance is achieved in all three different lumen diameters of (a) 0.23 mm, (b) 0.33 mm and (c) 0.43 mm. The Optical Lens View, shows the CTO as a white circle and the walls of the artery in grey. When saline concentration is lower than 98% the blood prevents the viewing of the CTO as shown in Figure. Here the clearance of blood and transparency of saline, give the clinician the view of the CTO.

3.5 Saline Flush Control and Regulation

Injection of saline into catheters involves the usage of a syringe or a syringe pump by an operator. The injection pressure is usually maintained by the continuous application of a constant force at the end of the plunger by the operator. In the diagnosis or treatment of CTOs, clinicians vary the position of the catheter with regards to the CTO before the flushing of blood takes place and the CTO is viewed. I. In such cases where the distance between the catheter and the CTO remains unascertained, it is likely that the catheter may come in close proximity of the CTO. While there may exist some clearance between the two, if the plaque encloses the catheter and CTO into a tiny region, the saline flushing process can create complications. There exists the possibility of a small, concentrated region of high pressure in front of the CTO which can risk either bursting of the diseased artery or uncontrolled disintegration of the CTO.

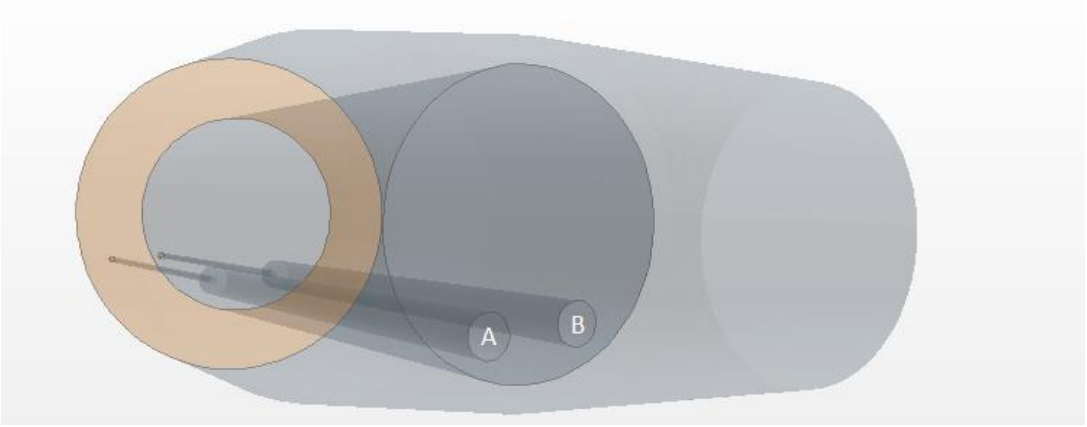

Figure 3.7 Geometric models of comparison of pressure vs mass flow control simulations. The suction (B) and injection lumens (A) were placed adjacent to each other to provide more space for additional elements of the catheter.

To understand the effects of the catheter at close proximity to the occlusion, two different saline injection techniques were investigated: Pressure-regulated vs mass flow-regulated saline injections. The primary difference involved in the two was synchronizing the suction and the injection mass flow rates to equal each other in the case of mass flow-regulated saline injection. This ensured that the amount of fluid (blood-saline mixture) moving through the outflow channel was the same as the amount of saline pumped into the artery. The results from the simulations provided interesting information. The pressure regulation applied at the ends of both the lumens created a small, compact region where a large overpressure of about 37 kPa developed. This is about three times the maximum blood pressure level that exists within a normal healthy coronary artery. In contrast, when mass flow control was used, the pressure dropped dramatically to about 13 kPa, due to the balance in the suction and injection. This change was simulated using constant velocity boundaries that mimicked the same mass flow rates, different from the case of pressure-regulated saline suction-injection.

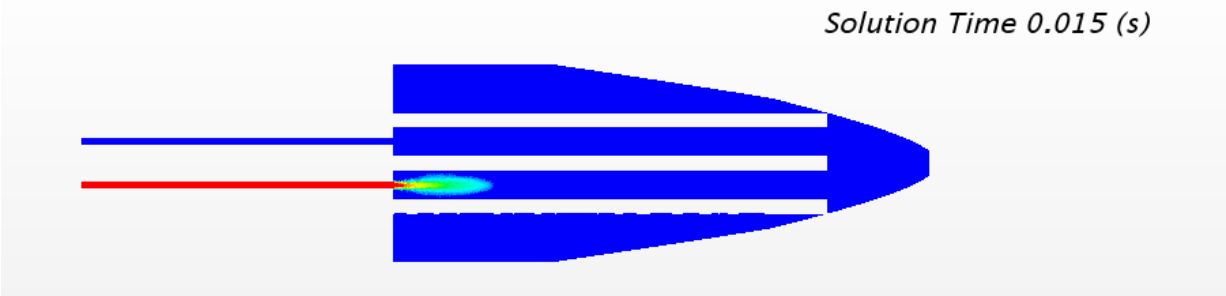
Solution Time 0.015 (s)

(a)

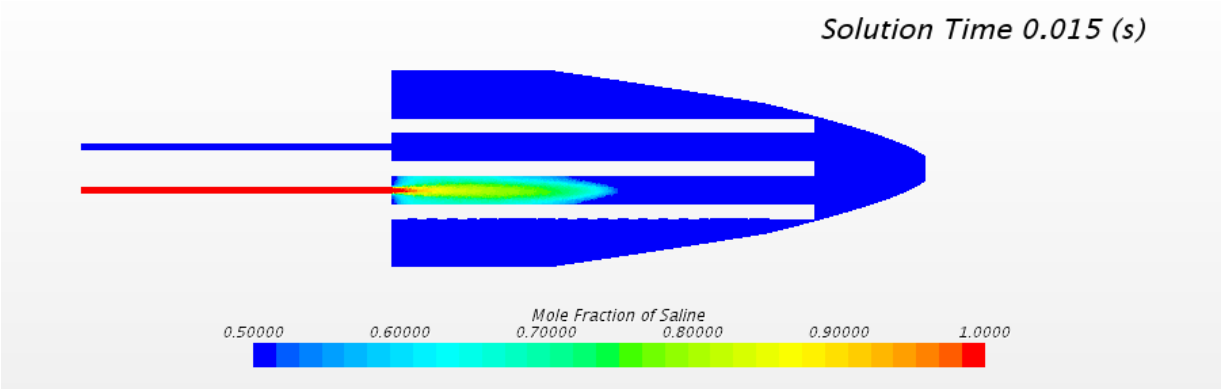
Solution Time 0.015 (s)
Mole Fraction of Saline
0.50000
0.60000
0.70000
0.80000
0.90000
1.0000

(b)

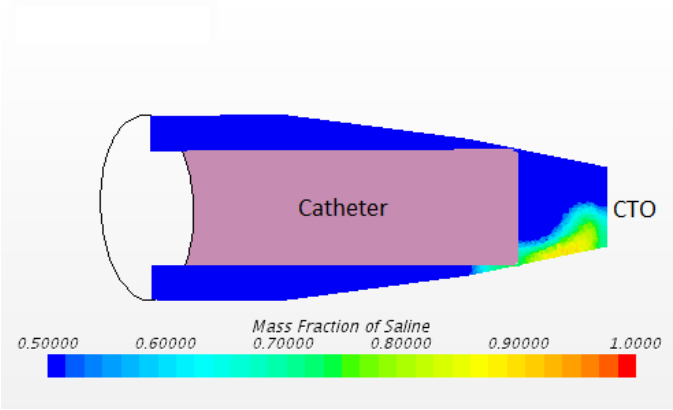
Catheter
CTO
Mass Fraction of Saline
0.50000
0.60000
0.70000
0.80000
0.90000
1.0000

(c)

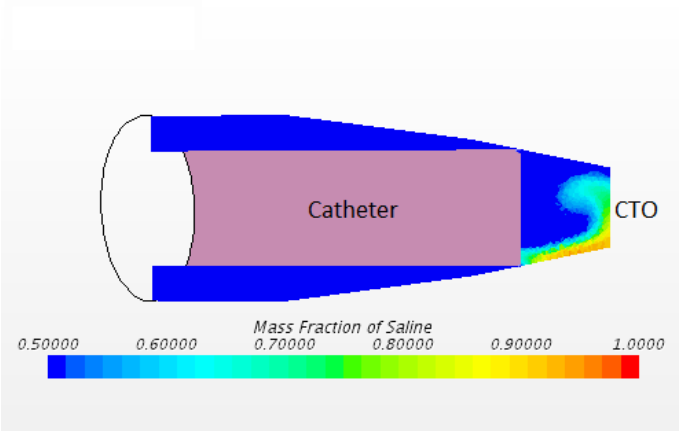

(d)

Figure 3.8 Saline injection flow patterns between pressure regulated and mass flow regulated catheters. The change in control type results in change in flow dynamics (a) Pressure controlled and (b) Velocity controlled. The flow patterns also get effected with some amount of saline leaking in (c) Pressure control, as compared to (d) Velocity control flow pattern

This has crucial significance, as the drastic reduction in pressure reduces the risks associated with the technique maintaining regular pressure levels within the diseased coronary artery. The time of flushing remained within acceptable limits, as the difference was under 2 seconds. The efficiency of suction also improved as the saline-blood mixture exiting via the outflow lumen increased to 95% from 60%, by changing the method of saline flushing to mass flow regulated instead of pressure regulation. By maintaining a fixed mass flow, the fluctuations due to external arterial blood flow in the saline inlet are also mitigated. This new technique of injecting saline and controlling the suction by harmonizing the flow rate in the two channels helps avoid unnecessary risk and complications that can possibly arise during the procedure. In cases where the synchronized suction injection catheter was used with a larger standoff distance in comparison with the adjacent lumen catheter clearance was achieved, however the flushing times increased by increased by 0.6 seconds and 0.46 seconds depending on standoff distances.

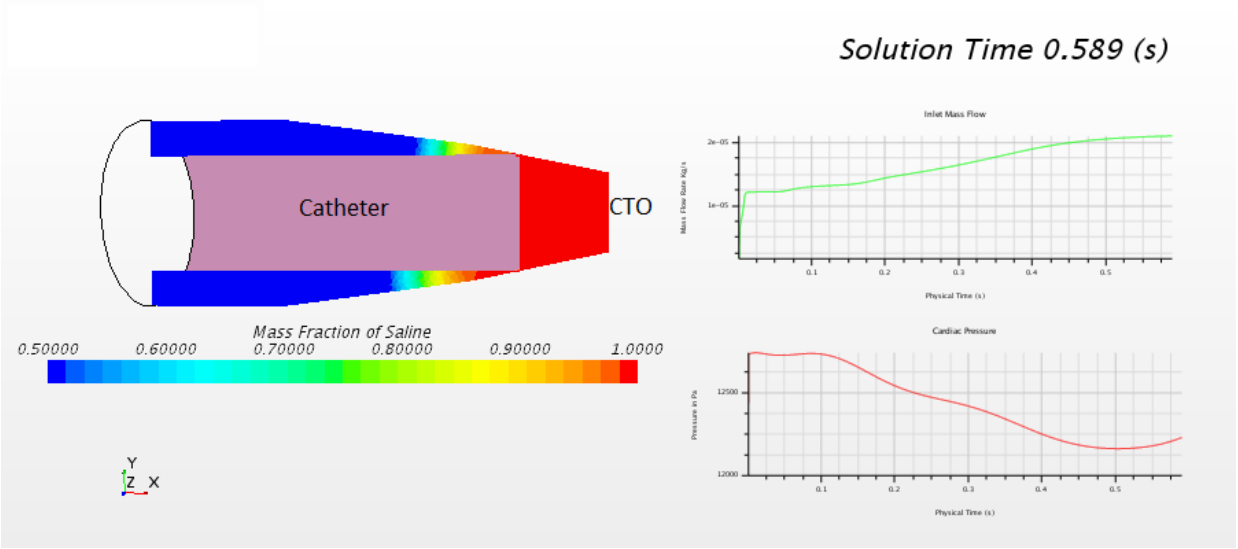
Solution Time 0.589 (s)
Catheter
CTO
Mass Fraction of Saline
0.50000
0.60000
0.70000
0.80000
0.90000
1.0000
Y
Z X
Inlet Mass Flow
Physical Time (s)
Cardiac Pressure
Physical Time (s)

(a)

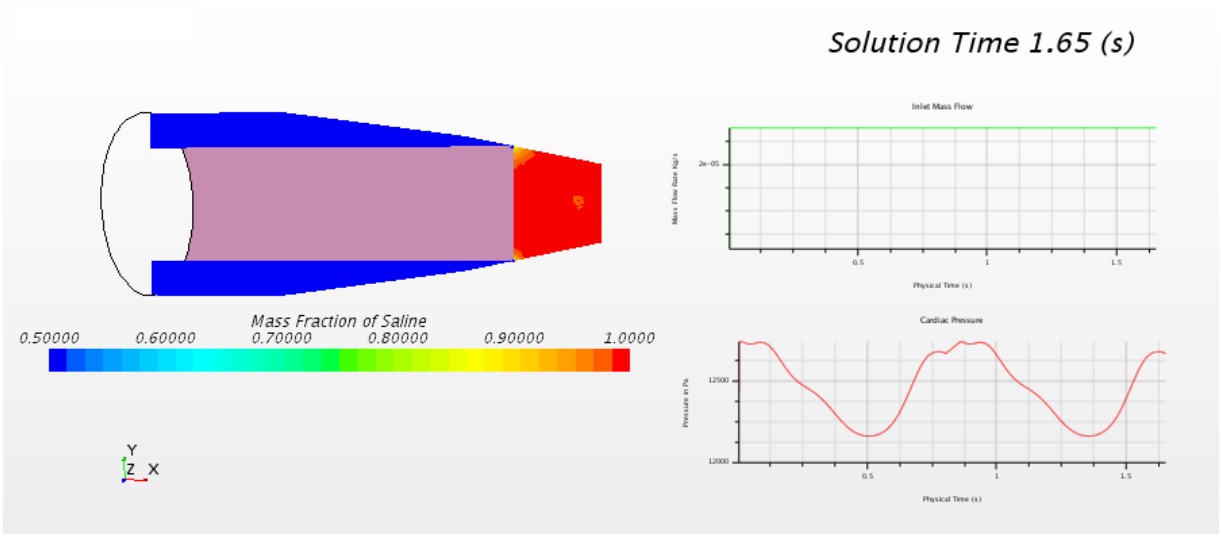
Solution Time 1.65 (s)
Mass Fraction of Saline
0.50000
0.60000
0.70000
0.80000
0.90000
1.0000
Y
Z X
Inlet Mass Flow
Physical Time (s)
Cardiac Pressure
Physical Time (s)

(b)

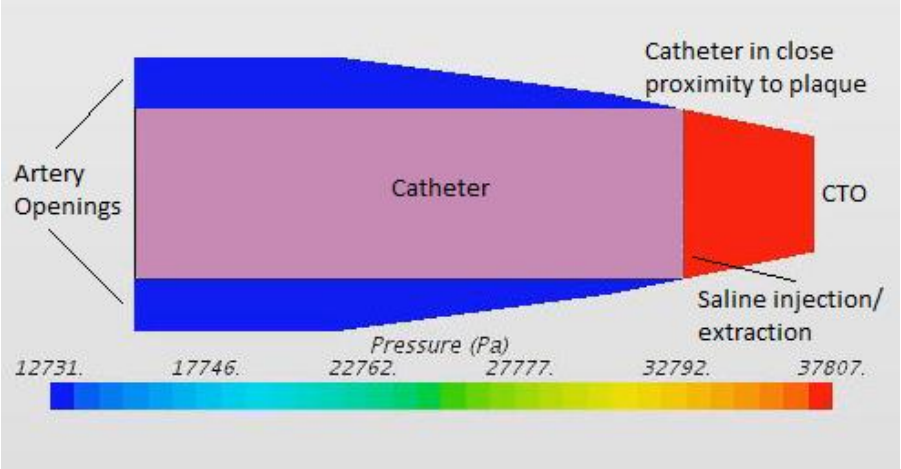

(c)

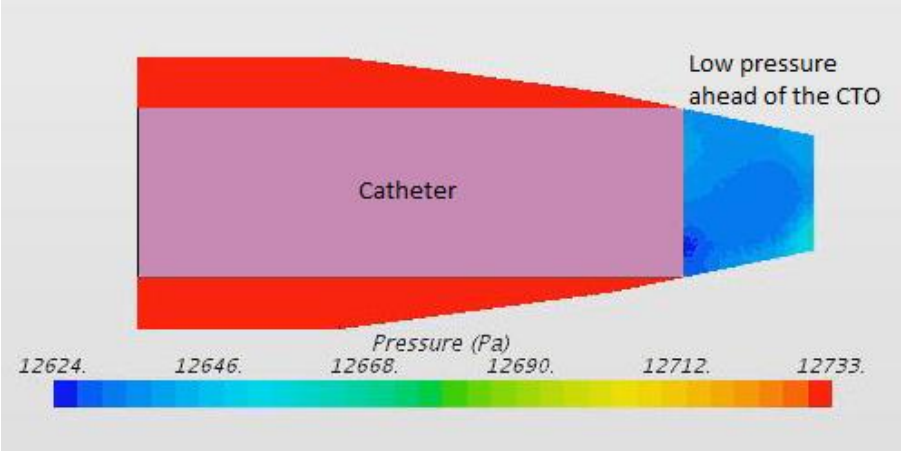

(d)

Figure 3.9. Comparison of mass fraction and pressure distribution in pressure vs mass flow regulation catheters. While clearance is achieved in both cases, the time difference is significantly larger in (b) velocity control as opposed to (a) pressure control. The results remarkably show that difference in the pressure distribution throughout the artery. In the case of (c) pressure control, pressures up to three times the normal arterial pressures are developed which are absent in (d) velocity control.

CHAPTER 4

ARTERIAL & PLAQUE MORPHOLOGIES

The human body is known to include a large degree of variations which are also seen inside the human circulatory system. The same blood vessel can have drastically different physical characteristics between different patients. Hence there is a need for the designed catheter to be able to function optimally under most CTO conditions. Atherosclerotic plaque is developed in not just the left anterior descending coronary artery but as well as neighboring arteries that exist such as the right coronary artery, left coronary artery and the circumflex artery. The catheters designed and developed need to be capable of function in a broad range of conditions to make them feasible within the industry. The catheters were thus tested in different morphologies of arteries, plaque build-up as well as external pressure conditions to understand how the functionality of the catheter may be affected by them.

4.1 Variations in artery and catheter sizes

The size of the arteries vary between different locations in the human circulatory system. The different artery sizes need to be accounted for in the design considerations of the catheter. The variability in the arterial size exists between different patients for the same artery. Different factors including genetics, lifestyle, eating habits, etc. influence the characteristics of blood vessels.

Hence, there is a need to establish the application of these catheters in varying arterial dimensions. To design a catheter which is feasible in these different artery sizes, the geometry of the artery model was changed.

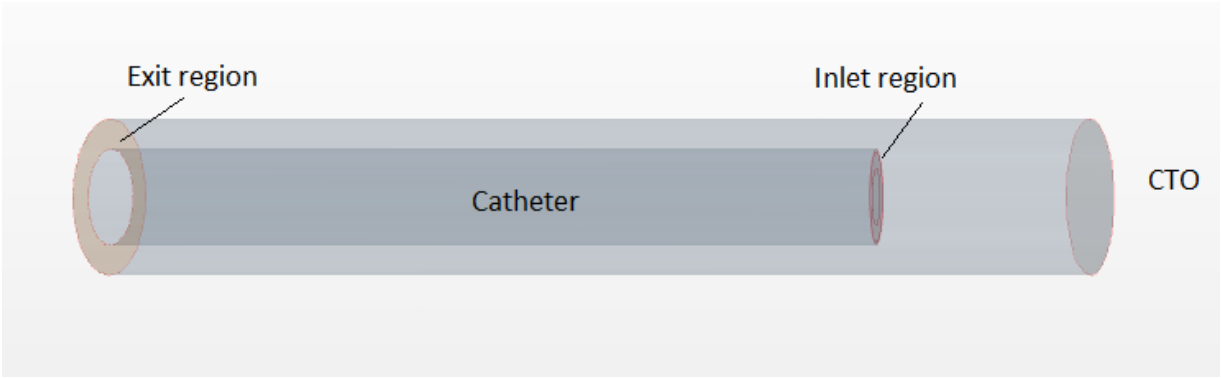

(a)

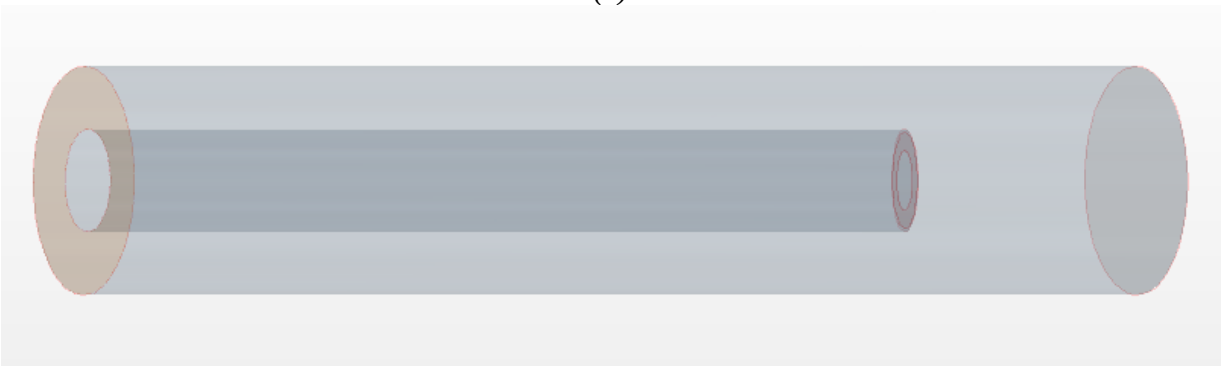

(b)

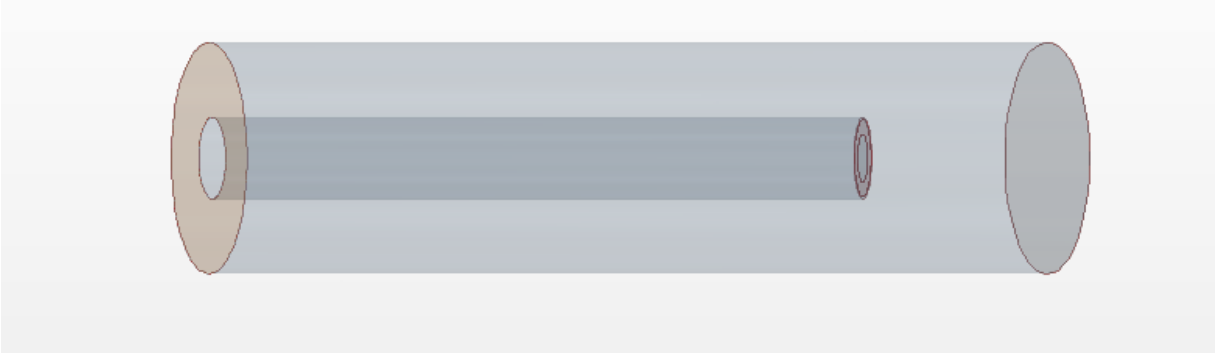

(c)

Figure 4.1 Different geometric models for arteries with varying diameters. (a) 2.7 mm (b) 3.7 mm (c) 4.7 mm. The red region denotes the saline injection, while the orange region represents the exit for blood and saline.

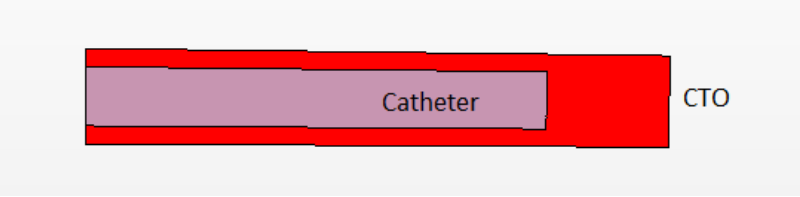

(a)

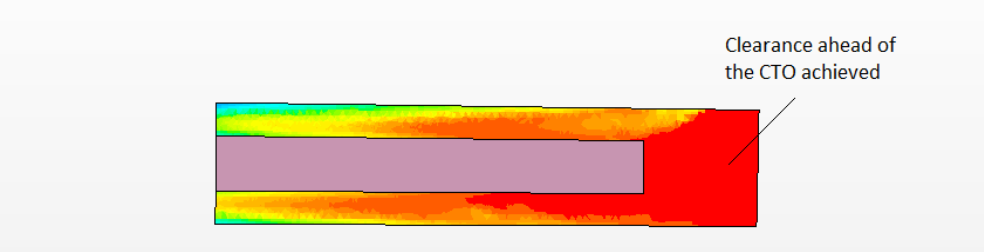

(b)

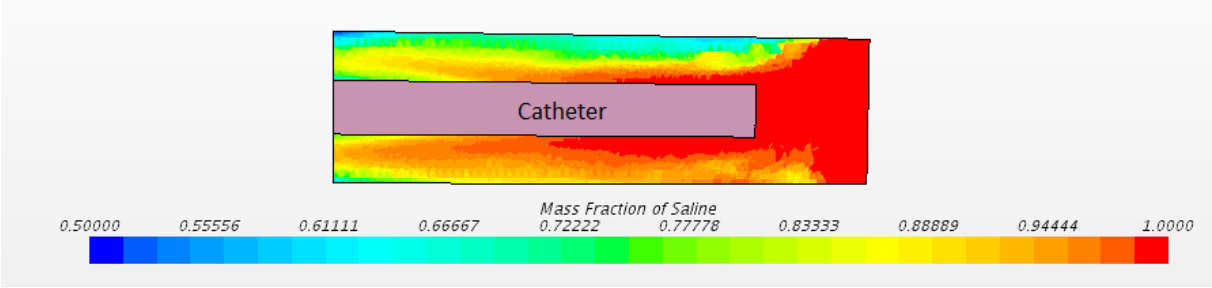

(c)

Figure 4.2 Showing clearance in different artery sizes. (a) 2.7 mm (b) 3.7 mm and (c) 4.7 mm diameter lengths for the respective arteries.

The annulus injection artery was used in the prediction of saline flushing in three different arterial diameters 2.7 mm, 3.7mm, and 4.7 mm. While saline flushing is achieved in all three as shown in Figure 4.2, the flushing mechanics change based on the clearance or space available between the catheter walls and the artery endothelium. In all three cases, the diameter of the catheter was fixed to 1.67 mm (5 French) and the saline flow rate remain unaltered. The resulting simulations showed that the time required for flushing reduces significantly as the artery size increases and then a slight

increase takes place with further increase of the arterial diameter, as seen in Table 4.1. This information suggests that there exists an optimum catheter to artery diameter ratio that can provide the fastest clearance in the artery.

Artery Radii	Time for flushing
2.7 mm	0.448 sec
3.7 mm	0.084 sec
4.7 mm	0.168 sec

Table 4.1 Showing the influence of the radius of the artery on time for flushing. A suitable catheter size may be needed to flush quickly in the absence of an auxiliary exit for the saline blood mixture.

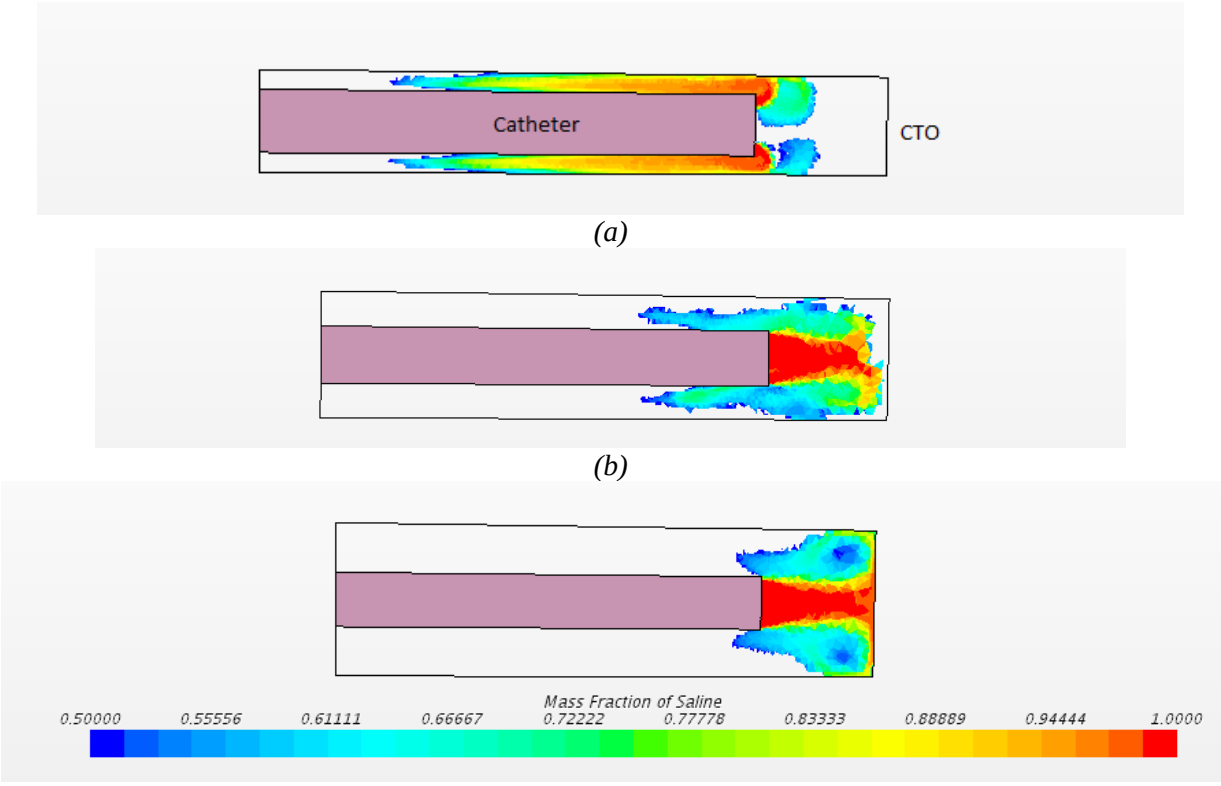

(a)

(b)

(c)

Figure 4.3 Different injection patterns for arteries of varying diameter. In (a) 2.7 mm the saline injection bends towards the exit and does not impinge on the CTO. Due to this the momentum of saline has a negligible effect in clearance. In (b) 3.7 mm and (c) 4.7 mm the saline jet merges from the annulus and uses its momentum to clear the region between the CTO and the catheter face.

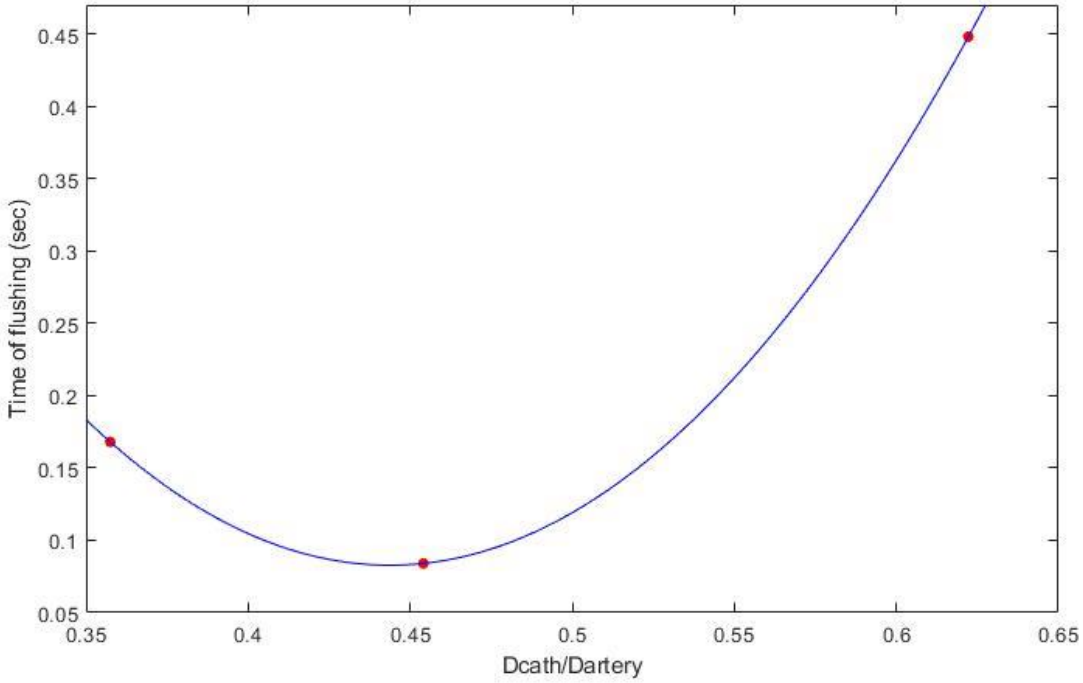

Figure 4.4 Optimum ratio for time of flushing in different arteries

Figure 4.4 shows the ratio of the catheter diameter to diameter of the artery with the time of required for flushing. The optimum ratio is about 0.45 for the given saline flow rate, which implies that the diameter of the artery is double the catheter diameter and the clearance between the two is about the length of one radius of the catheter face. The significance of this optimum ratio rises in future designs of the catheter where suction is introduced such that, in the absence of any exit lumen for the blood-saline mixture, sufficient clearance is crucial between the artery and the catheter. As seen in Figure 4.3a), the flow of saline begins to flail about the catheter edge instead of being projected towards the CTO. This low momentum flow fails to clear out the blood. With the same flow rate, the flushing mechanism is widely different: the mixing of saline into blood begins to dilute the mixture and provide clearance, as opposed to using its momentum to push out

the blood away from the CTO, as it is unable to hit the CTO as a saline jet issuing from the catheter tip. In contrast, as this ratio is reduced, the saline injected into the artery is able to jet across the standoff volume, and push the blood away from the region of interest to obtain clearance immediately.

4.2 Curved Artery

The coronary arteries are named as they rest around the heart in the shape of a crown. Major sections of these arteries are curved and some are extremely tortuous leading to difficulty in their treatment. In reality, none of the coronary arteries have straight sections where atherosclerotic plaque develops. The coronary arteries tend to bend over the cardiac muscle so as to envelop the heart and provide oxygenated blood to it. Hence, there existed a need to prove the validity of the study for practical cases and that the simulation models will hold when representing the anatomy of arteries in actual diagnosis. A curved artery was constructed and the catheter was made to take a curved route to reach the proximal end of the CTO. The geometry is designed such that the catheter is driven all the way to one edge of the artery, due to which an offset exists between the catheter and the arterial axes. The saline flow rate is maintained at 2 cc/sec. The annulus lumen provides a swirling injection into the artery, which results in certain amount of saline not utilized completely in clearance of the blood. Despite the waste of some saline, clearance is entirely achieved shortly after injection. The successful clearance of blood shows that these simulations using the proposed catheter design will remain valid for varied geometries of the arteries.

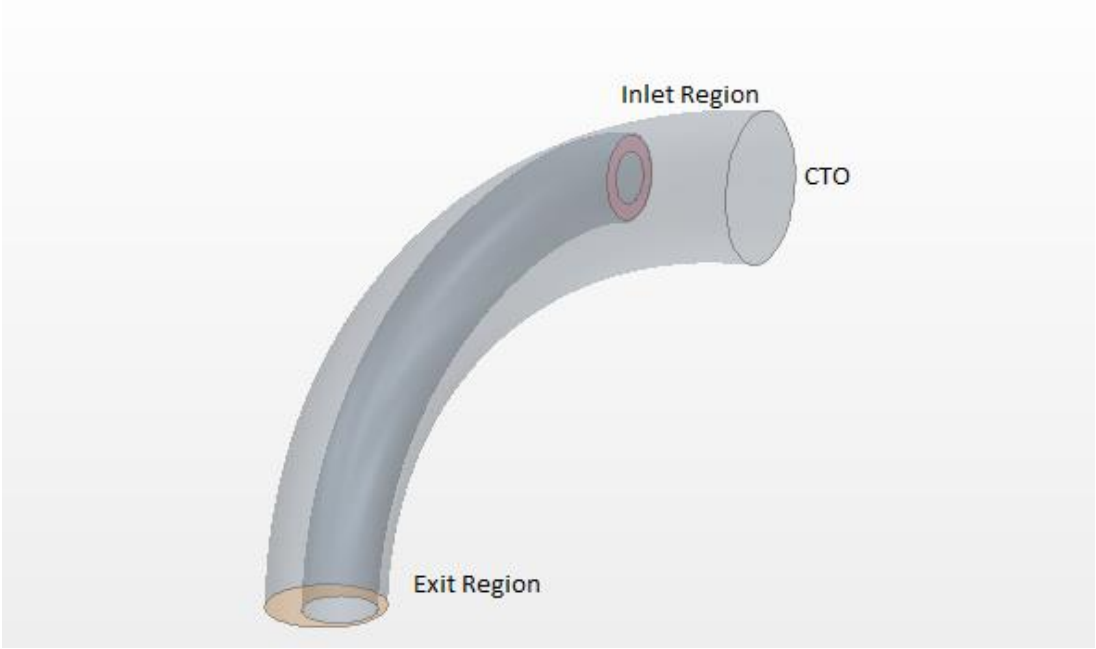
Inlet Region
CTO
Exit Region

(a)

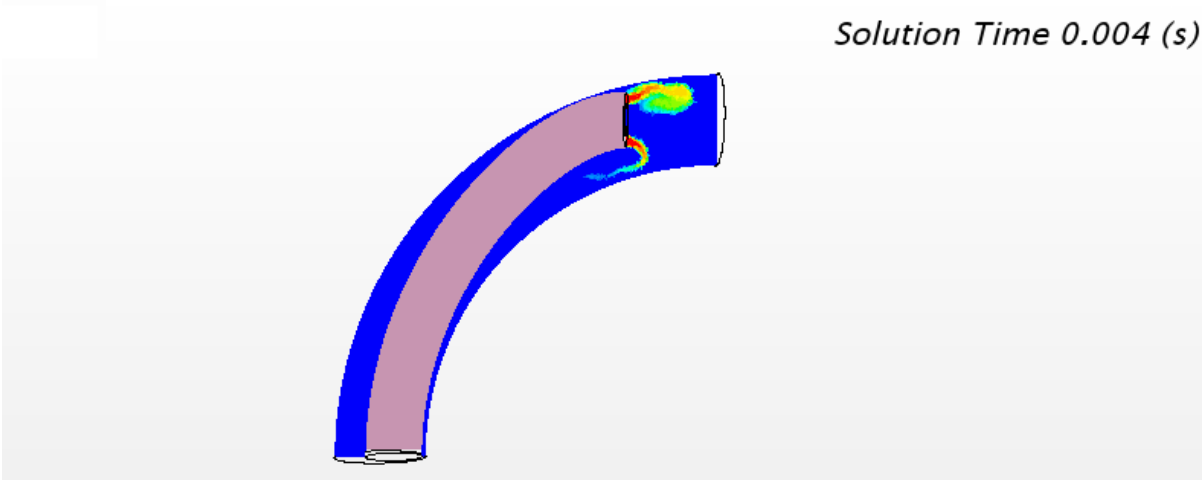
Solution Time 0.004 (s)

(b)

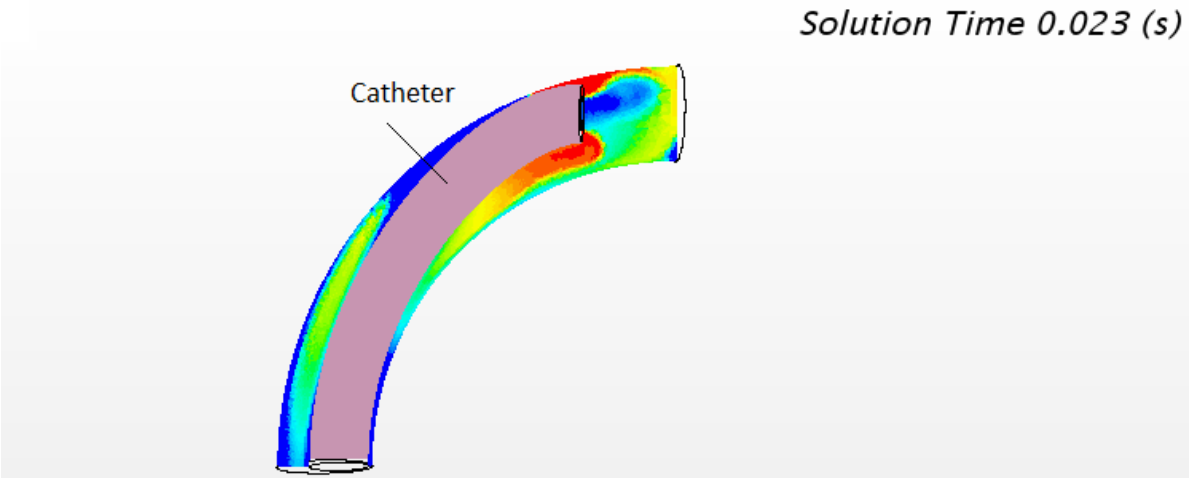
Solution Time 0.023 (s)
Catheter

(c)

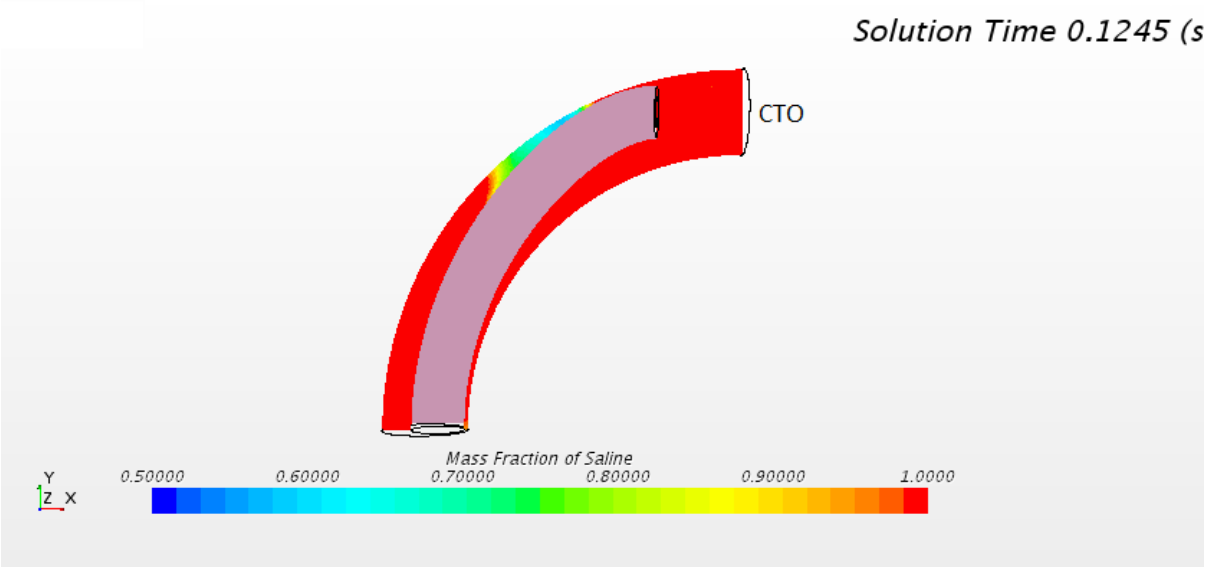

(d)

Figure 4.5 Curved artery simulation results. The outer curved section in (a) represents the model of a curved artery. The catheter tubes are extremely flexible and are driven to the side of the artery wall ahead of the CTO. The injection region is denoted by red and the outflow for saline and blood is colored orange. When saline is injected into the artery (b) the upper portion of the jet moves ahead while the lower portion moves towards the outflow. About half the saline injected (c) remains un-utilized as seen in the flow patterns. (d) shows that clearance is easily achieved in curved arteries with the design as well.

4.3 External blood Pressure

In some cases, during actual surgical operations the distal opening of the artery is occluded using a balloon to prevent the entry of fresh blood pumped from the heart. The balloon usually occludes the entire lumen, but sometimes a small gap may persist between the balloon membrane and the artery walls. There are other procedures where the balloon occlusion is avoided, to prevent any damage to the arterial endothelial layer. In such a case, blood pumped from the heart continues to enter into the region between the catheter tip and the CTO, interfering with the saline flushing process. Additionally, this creates a pressure imbalance within the artery for saline infusion. The

injecting pressure of saline must be higher than the neighboring blood pressure, to be able to penetrate and push the blood away, as well as to avoid the blood from entering the saline injection lumen. To simulate this, coronary artery blood pressure was adopted from previously published literature. The extracted pressure wave was then processed and repeated to create a cyclic effect as observed within the coronary arteries.

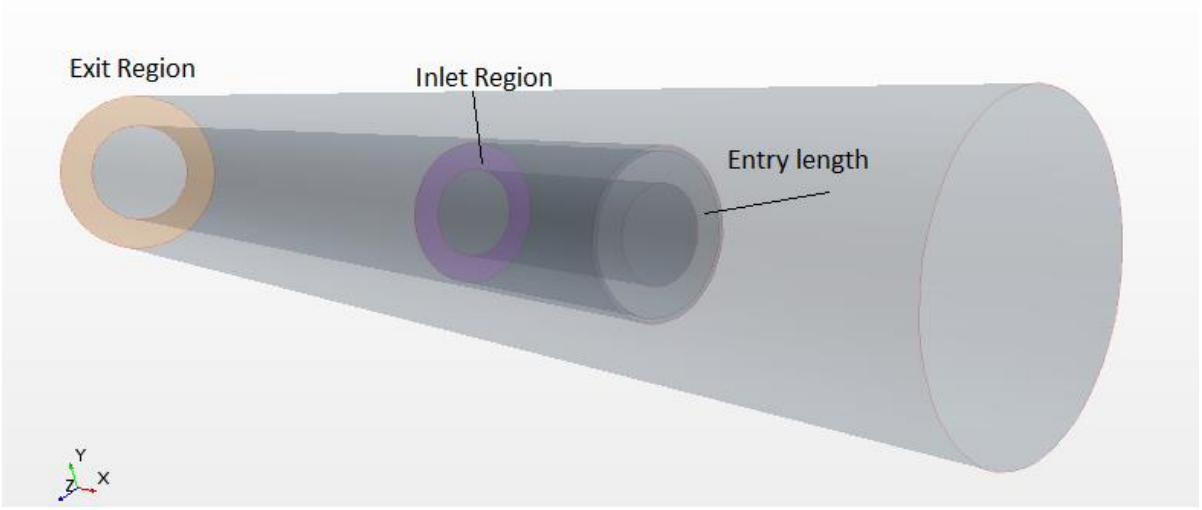

Figure 4.6 Simulation model for incorporating external blood pressure. The geometric model used for the predicting saline flushing under blood pressure from the heart. The arterial blood pressure is applied at the region highlighted in orange. The pressures required for saline injection need to be higher than this pressure to enable the flow of saline blood mixture via the same arterial opening. An entry length is provided to create a developed flow before saline injection.

To accommodate for the new external blood pressure, pressure injected into the catheter is required to overcome the arterial blood pressure at every time in the blood pressure cycle. The arterial blood pressure describes the initial pressure within the entire domain and affects the pressure downstream of the saline injection lumen. Additionally, in these simulations, a length of ten times the lumen diameter was provided as an entry length in order to create a fully developed flow of saline before being introduced into the artery.

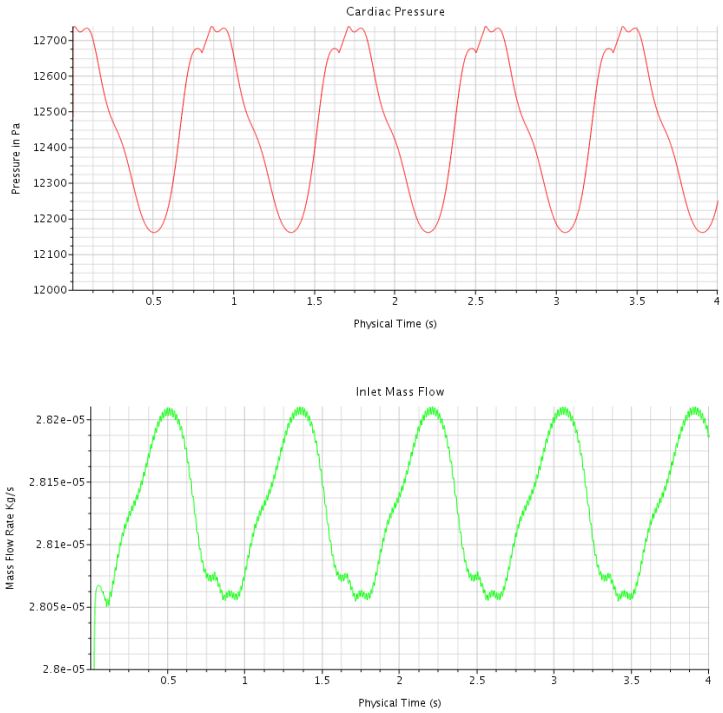

Figure 4.7 Influence of cardiac pressure (top) on the effect of mass flow of saline injection into the artery (below)

The pressure variation due to the arterial blood flow, results in continuous changes in the pressure difference between the injection and the outflow of the saline blood mixture. This results in a fluctuating injection mass flow rate of saline into the artery. This effect is predominant where saline injection is regulated using pressure as opposed to regulation via the mass flow (see section 3.5).

Time of Injection	Average Mass Flow	Time for flushing
Start of Systole	1.15 cc/sec	1.41 sec
Before Systolic Peak	1.10 cc/sec	1.50 sec
After Systolic Peak	1.14 cc/sec	1.57 sec

Table 4.2 The effect of arterial pressure is large in the saline flushing mechanics. However, by varying different time of injection, the changes in flushing time are minimal.

As shown in Table 4.2 the injection timing was analyzed for three different scenarios namely; at the start of systole, right before the systolic peak and right after the systolic peak. The timings of the pressure inside the coronary artery are out of phase with the heart due to the leaflets at the aortic opening. The longest time required to flush the artery takes place when saline is injected right after the systolic peak, while the shortest clearance time is when the saline is injected right at the start of systole. While the difference in timing is small, in catheters where synchronizing the injection timing to the heart beat is possible, this would help elucidate the optimum time to start saline inflow and efficiently clear out the blood.

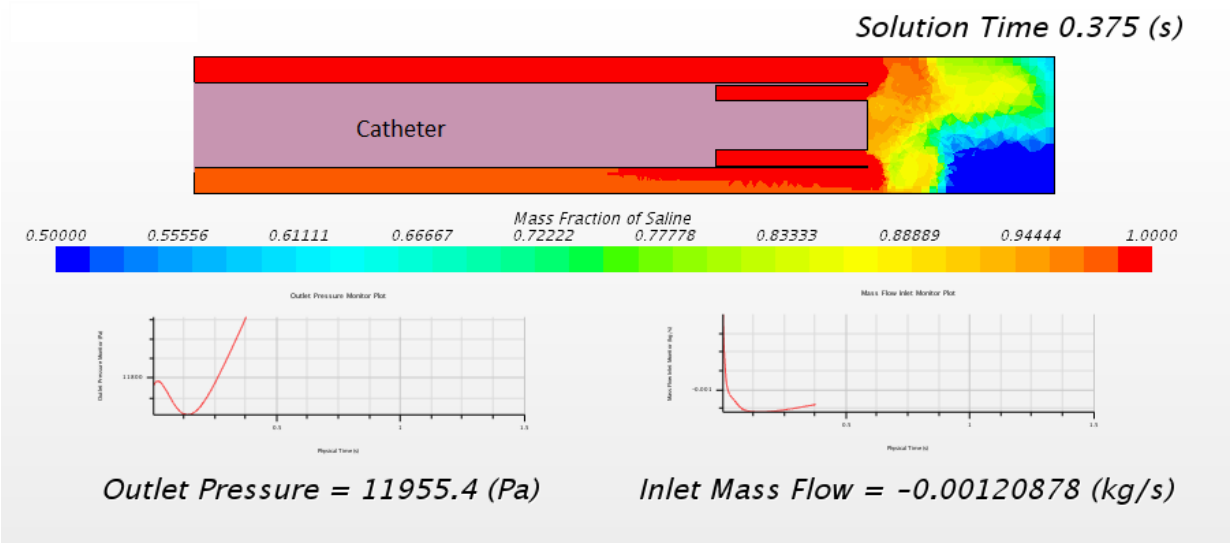

(a)

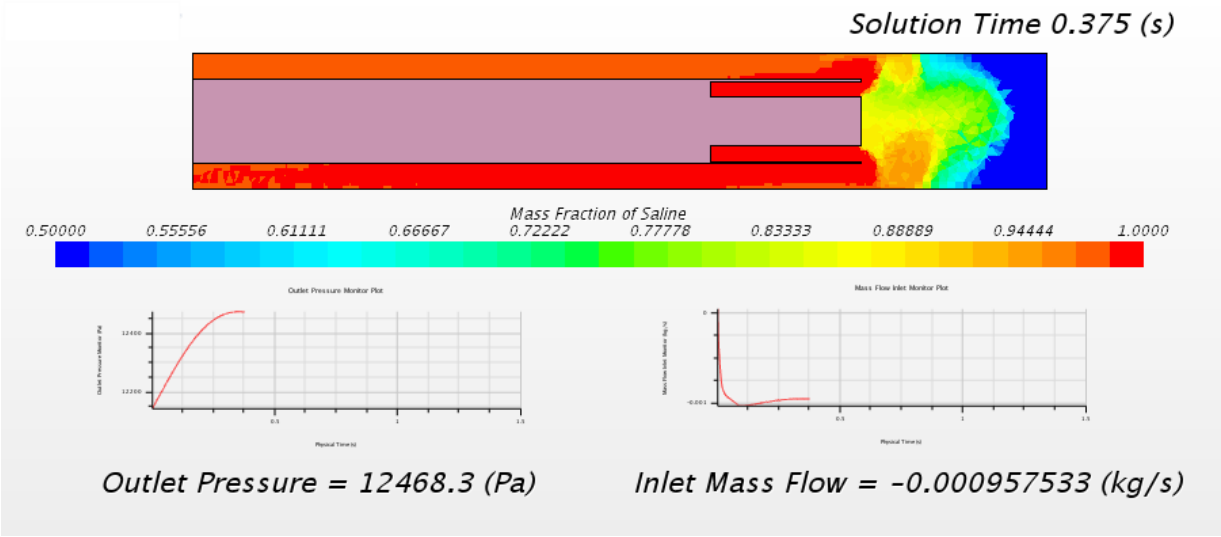
Solution Time 0.375 (s)
Mass Fraction of Saline
0.50000
0.55556
0.61111
0.66667
0.72222
0.77778
0.83333
0.88889
0.94444
1.0000
Outlet Pressure = 12468.3 (Pa)
Inlet Mass Flow = -0.000957533 (kg/s)

(b)

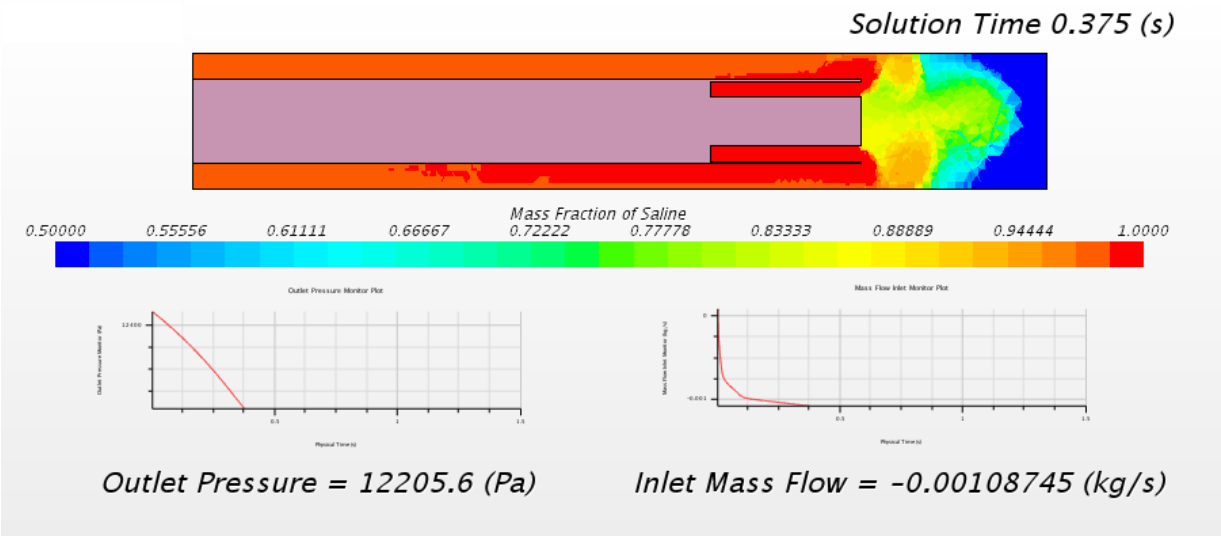
Solution Time 0.375 (s)
Mass Fraction of Saline
0.50000
0.55556
0.61111
0.66667
0.72222
0.77778
0.83333
0.88889
0.94444
1.0000
Outlet Pressure = 12205.6 (Pa)
Inlet Mass Flow = -0.00108745 (kg/s)

(c)

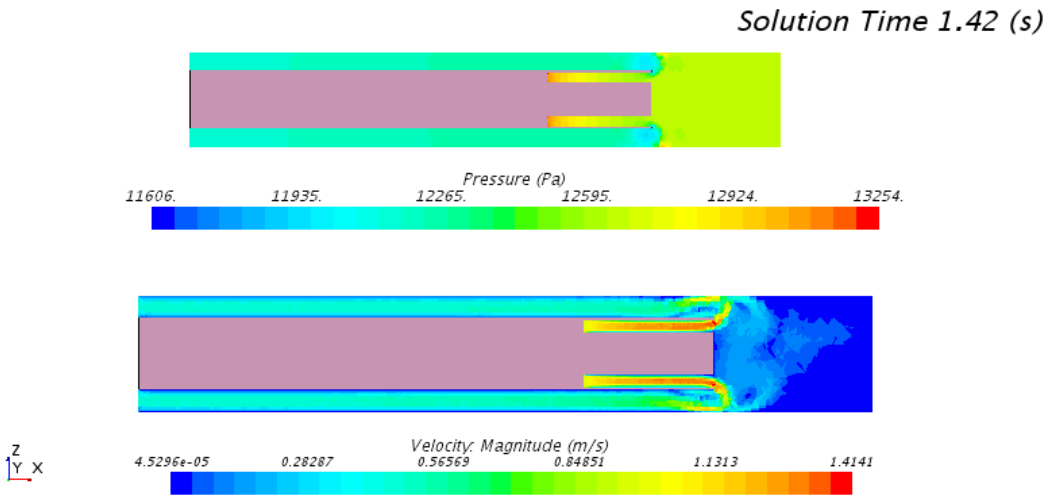

(d)

Figure 4.8 Flow patterns under the application of blood pumped from the heart. The flushing patterns are sightly different at a given (a) start of systole, (b) before systolic peak and (c) after systolic peak due to differences in timing with respect to the arterial pressure wave. The negative sign in the inlet mass flow is due to the frame of reference. The flow velocity and presure distribution required to flush the blood (d) inside the artery is shown.

4.4 Varying Plaque Morphologies

CTOs generally are not stand-alone diseases and are often found next to growing atherosclerotic plaque buildup. The development of the plaque may be negligible resulting in a sudden stenosis. Generally, there is a gradual development of plaque inside the artery, which continues to grow resulting in the complete occlusion of the artery, forming the CTO. The development of the CTO is influenced by a large number of factors such as genetics, previous history of cardiovascular diseases, age, lifestyle choices etc. To predict the outcome of the flushing techniques three different CTO upstream conditions that may arise were studied sequentially. Three different primary geometries were created and flushing in them was simulated. Simultaneously, the suction

lumen and the saline injection channel were placed adjacent to one another to replicate newer ideas for the design of the catheter. The inherent advantage of such a design is a significantly larger section of the catheter becomes available for instruments, while the two lumens are held next to one another inside the catheter body.

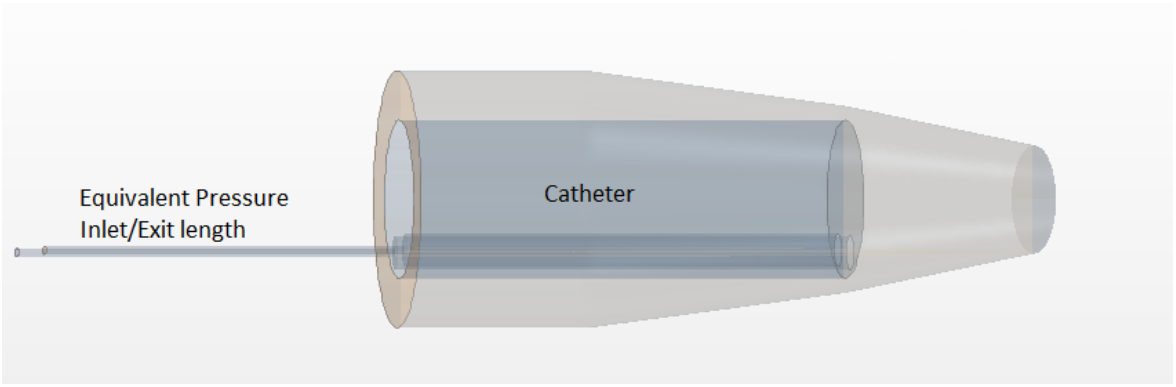

(a)

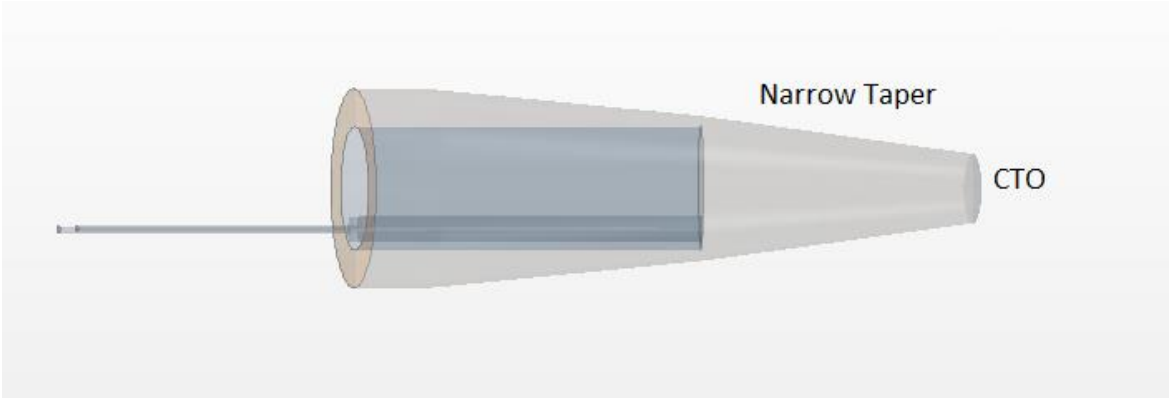

(b)

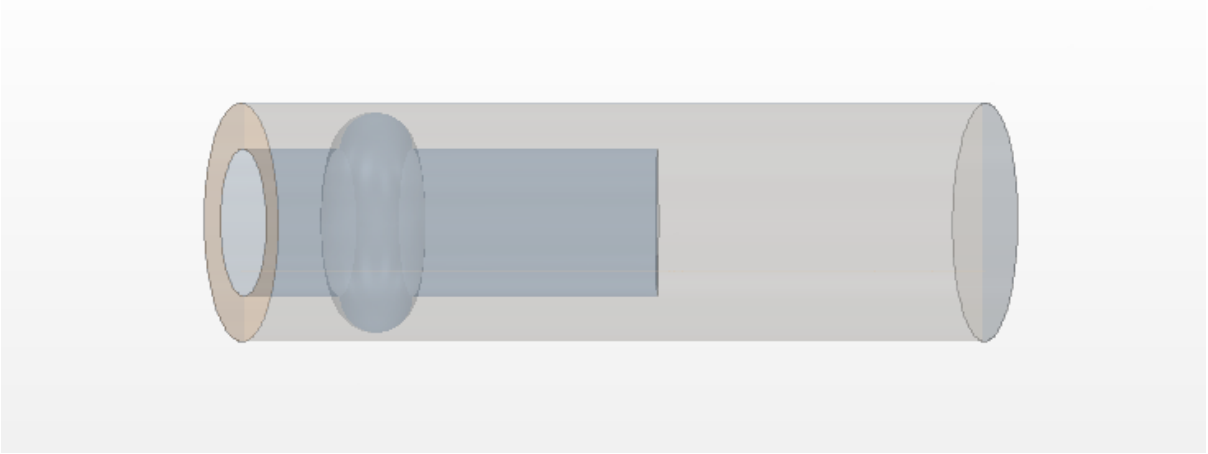

(c)

Figure 4.9 The geometric models for different plaque morphologies. Displaying the differences between the plaque morphologies (a) steep taper (10^0), (b) shallow taper (5^0), and (c) with zero taper due to negligible plaque buildup. The extend tubes before the injection of saline are introduced to simulated the pressure drop about 1m length, between the injection of saline by the clinician and the site of the CTO.

The plaque morphologies were created with a 5^0 angle representing a shallow taper, a 10^0 angle designating a steep taper, and a straight section showing negligible plaque accumulation ahead of the CTO. The standoff distance between the catheter and the CTO was either 0.2 mm or 0.4 mm. The lumen diameters for the saline inflow and outflow channels were 0.35 mm and 0.25 mm for each morphological case.

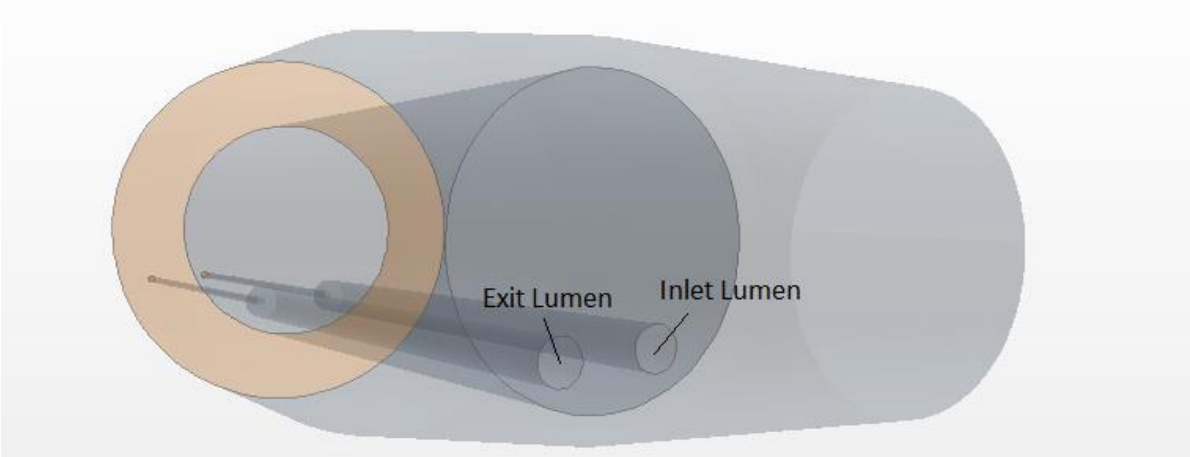

(a)

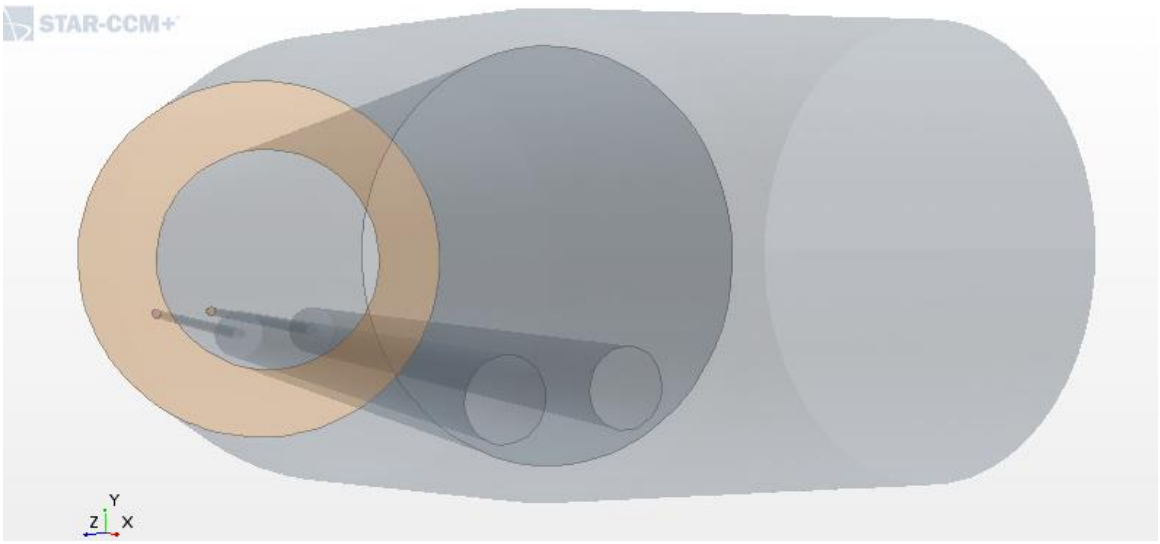

(b)

Figure 4.10 Variation of lumen diameters.(a) 0.25 mm and (b) 0.35 mm.

Instead of calculating the pressure drop across the catheter face and presumed saline inlet, while injecting saline an equivalent pressure tube was designed inside the catheter. The pressure at the inlet was now maintained at 100 kPa which resulted in saline mass flow rates of 0.0086 cc/sec and 0.0280 cc/sec in the 0.25 mm and 0.35 mm lumens respectively. The total volume ahead of the CTO which required to be flushed was 20 mm^3 and 30 mm^3 in the shallow taper and the straight section respectively. In addition, the standoff distance for the steep taper or wedge 1 is reduced to imitate a surgical flushing where the distance between the catheter and the CTO is unknown to the doctor prior to saline flushing and diagnosis.

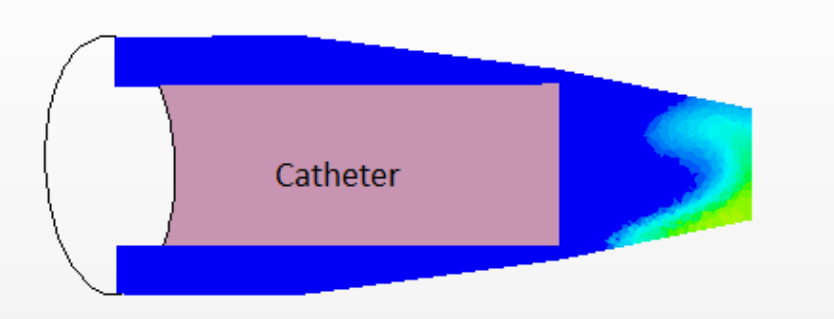

(a)

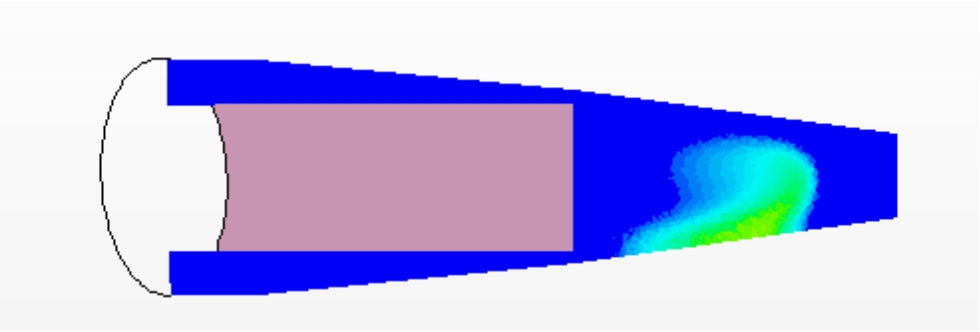

(b)

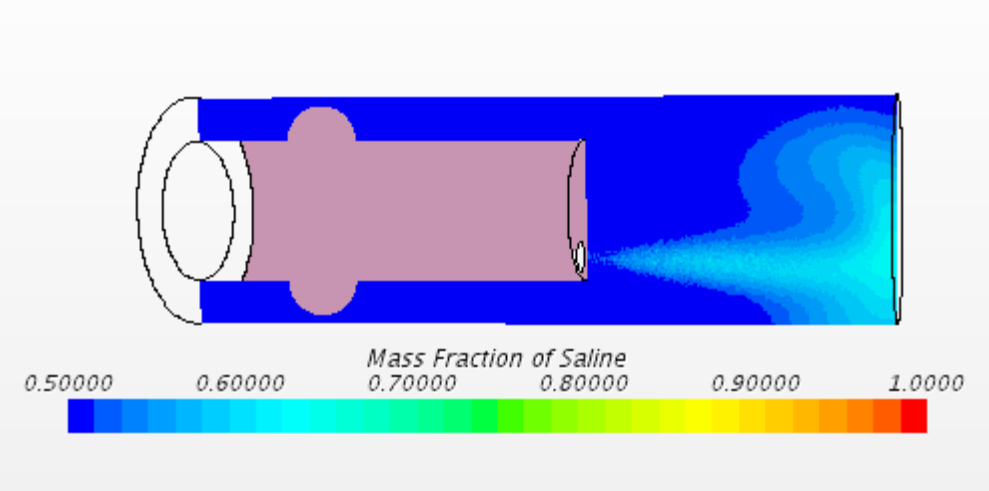

(c)

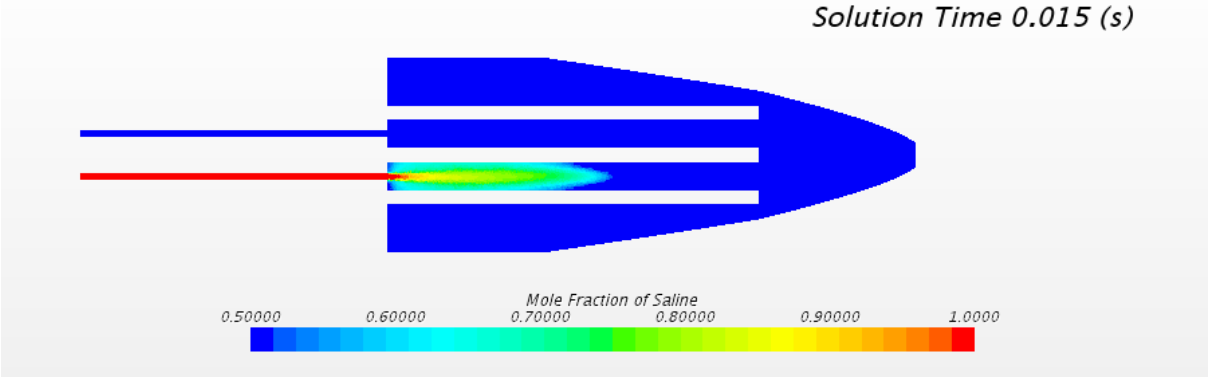

(d)

Figure 4.11 Flow patterns for different plaque morphologies. The inlet flow patterns for the same saline injection rates in the different plaque morphologies (a) Steep Taper, (b) Narrow Taper, and (c) Zero Taper is found to be different. The saline injection via the new pressure equivalent tubes is shown in (d).

Clearance is achieved in each morphological case as shown in the Figure 4.11. Table 4.3 shows the results of the simulations, where the longest flushing time, equal to 8 seconds, occurs for the case of the straight section. This longer time is mainly due to the large standoff distance between the catheter tip and the CTO. By reducing this distance, the time of flushing can be dropped as desired. The minimum flushing time was less than a second, for the case of wedge 1 which represents the smallest stand-off volume.

Geometry	Flowrate	Velocity	Re	Inlet Pressure at catheter face	Time for Flush
Wedge 1 (0.35mm)	0.028 cc/sec	0.291 m/s	114	88 kPa	0.7 sec
Wedge 1 (0.25mm)	0.0086 cc/sec	0.176 m/s	50	95 kPa	1.9 sec
Wedge 2 (0.35mm)	0.028 cc/sec	0.291 m/s	114	88 kPa	1.0 sec
Wedge 2 (0.25mm)	0.0086 cc/sec	0.176 m/s	50	95 kPa	4.1 sec
Straight (0.35 mm)	0.0275 cc/sec	0.285 m/s	112	90 kPa	3.2 sec
Straight (0.25mm)	0.0086 cc/sec	0.175 m/s	50	95 kPa	8.7 sec

Table 4.3 Clearance is achieved for different geometries and different lumen diameters while the time of flushing remains within practical intervals.

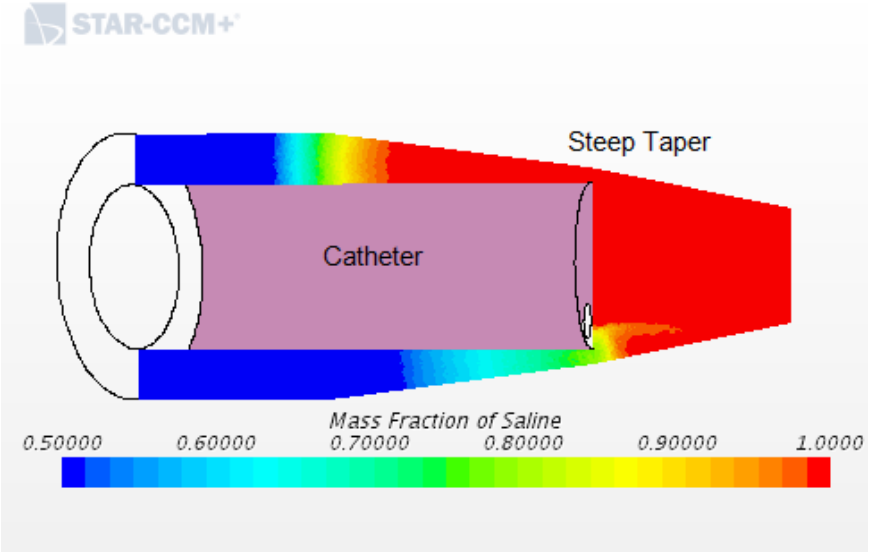

(a)

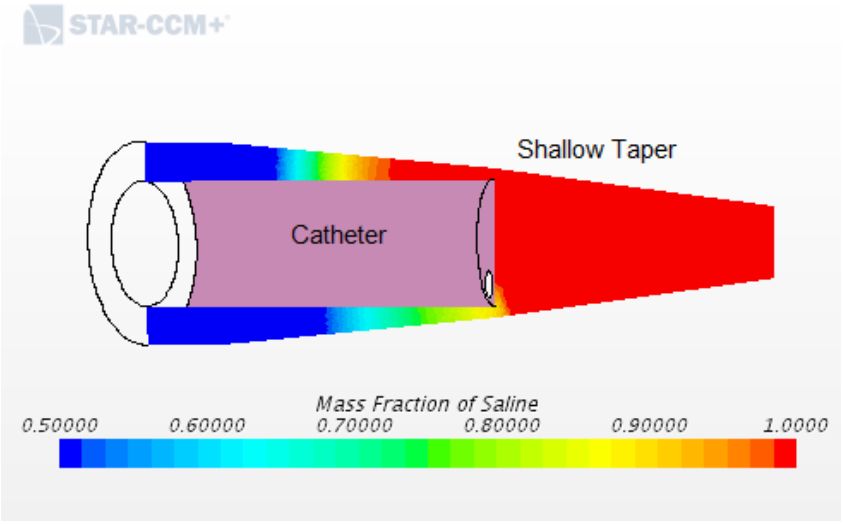

(b)

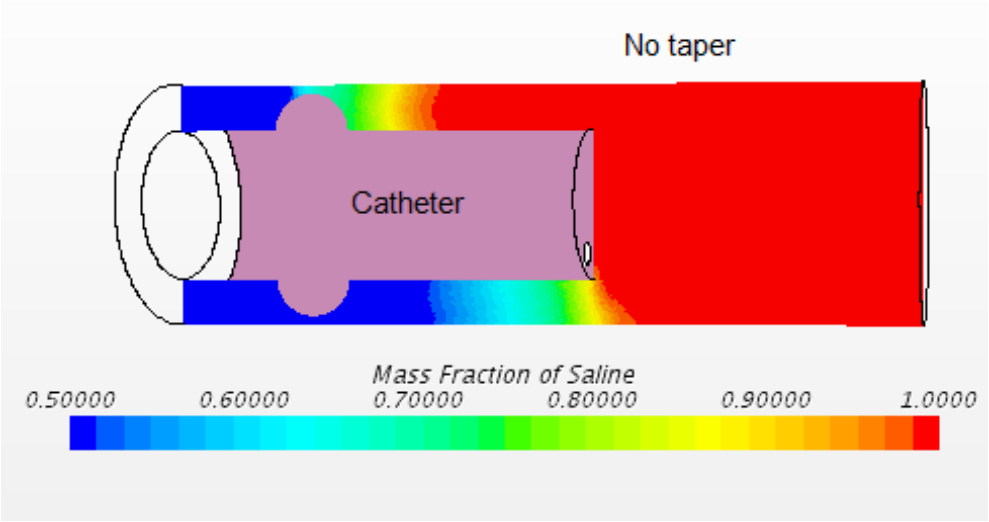

(c)

Figure 4.12 Clearance in different plaque morphologies. Plaque development dependent of different factors takes place in the form of different geometries. The different geometries simulated (a) Steep taper (10º), (b) Shallow taper (5º), and (c) No taper. Clearance can be achieved in all cases for different lumen diameters

4.5 Influence of Hematocrit on fluid mechanics

As saline is injected into the artery, it dilutes the blood and changes the properties of the fluid mixture. One of the major changes that take place within the blood properties is the hematocrit.

The hematocrit influences different properties of blood, and in particular the viscosity of blood. For flow in large vessels, there exists a non-linear relationship between hematocrit and viscosity. Existing data from published literature was incorporated in the simulation to understand how the change in hematocrit and viscosity affect the flushing times and the saline flushing technique.[30]

Morphology	Constant Viscosity	Hematocrit influenced viscosity
Steep Taper	0.58 sec	0.61 sec
Narrow Taper	0.99 sec	0.97 sec

Table 4.4 The influence of varying viscosity on clearance times of blood.

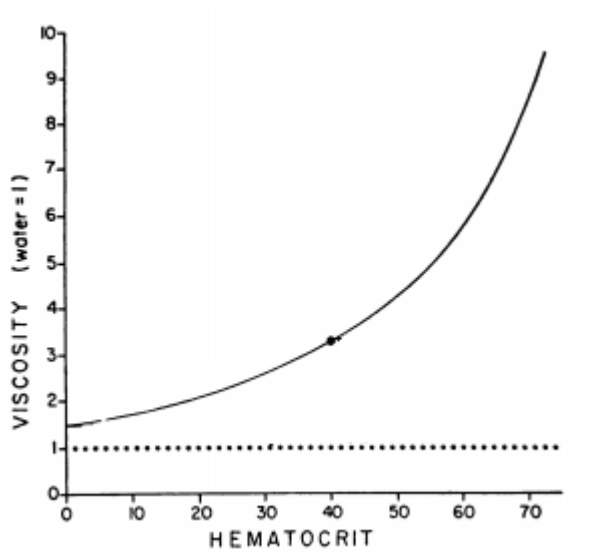

Figure 4.13 The influence of hematocrit on the viscosity of the blood.[30]

While the viscosity effect of the saline solution mixing into blood was considered, its influence on flushing time was found to be negligible. In the two trial cases, the difference when using a hematocrit-dependent blood viscosity in the simulations resulted in a flushing time difference of about 0.03 seconds. However, this difference remains inconsistent between different simulations, with no definite pattern amongst them.

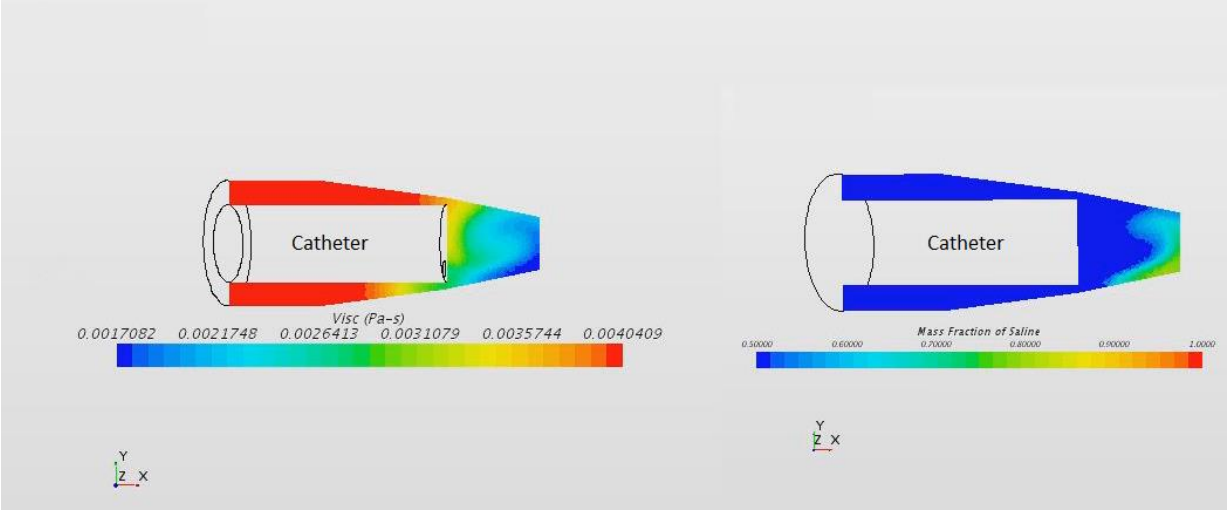

(a)

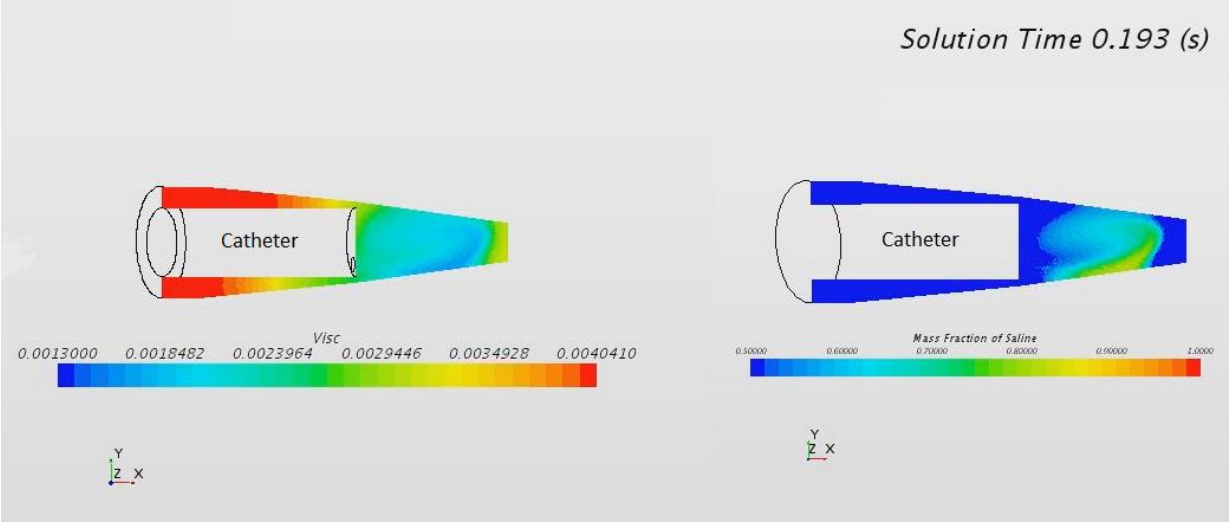

(b)

Figure 4.14 Varying viscosity due to dilution of blood and changing hematocrit. The injection of saline dilutes the blood mixture resulting in changing the hematocrit and the viscosity of the mixture. The viscosity of the fluid is depicted on the left and the saline injected into the artery is shown in the right.

CHAPTER 5

OPTICAL ANALYSIS

During the technique of saline flushing, the saline solution mixes with blood. As saline pushes the blood, the overall mixture increases its transparency to light. While the fluid simulations provide a good understanding of the physics of the flow of saline and blood, to visualize the CTO for treatment, it is required to understand the physics of light propagation through the saline and blood mixture while flushing takes place. An optical analysis was conducted in the study, to investigate whether the catheters designed are capable of providing complete visualization of the CTO, while providing insight into the characteristics of the mixture transparency. The optical analysis provides additional confidence in simulations where clearance was qualitatively computed earlier. This enables the recommendation of different catheter designs that can be used for flushing blood and treating patients with CTOs.

The visibility of CTO was depicted in the study using a blue and white checkered target. As the blood is diluted, its transparency increases resulting in the successful visualization of the target. At 80 percent visibility, the red hue of the blood is minimal and the blue can be distinguished from the adjacent white on the target. At this visibility, the blood essentially allows for about 90 percent of the light to pass through in one direction and a cumulative amount of about 80 percent returns to the receiving optical lens after reflection from the CTO. The flushing time values obtained from the optical analysis were compared with the qualitative images obtained from the simulation study.

There is good agreement between the qualitative analysis of clearance and the optical study to identify actual clearance times during this technique.

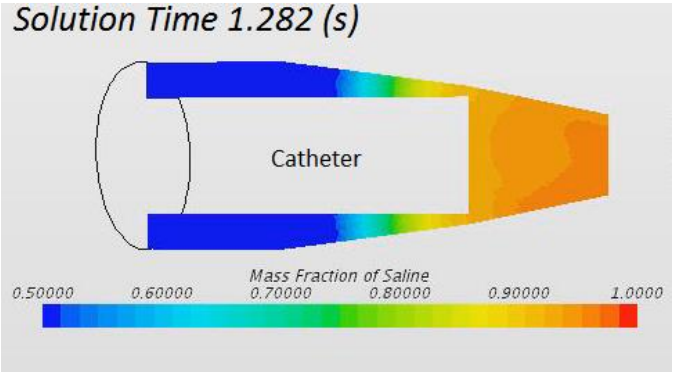

(a)

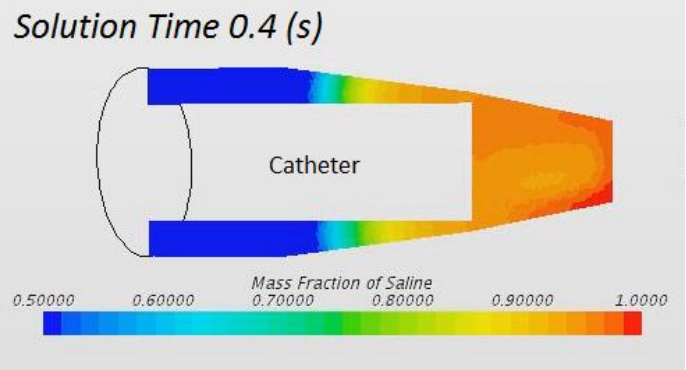

(b)

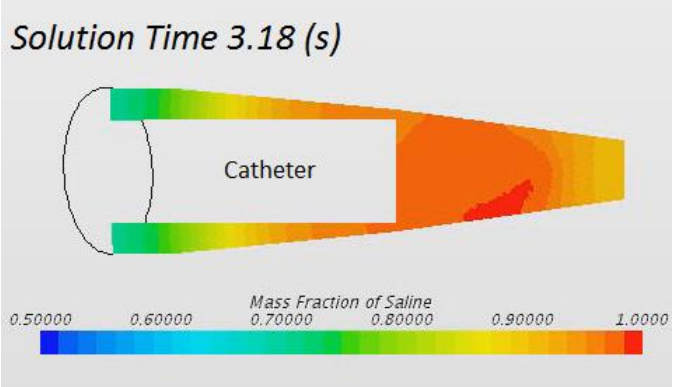

(c)

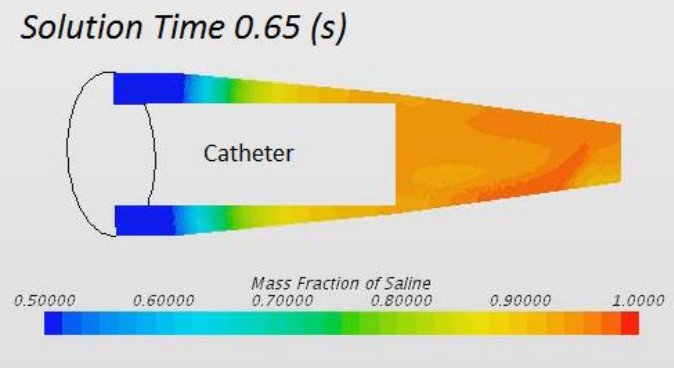

(d)

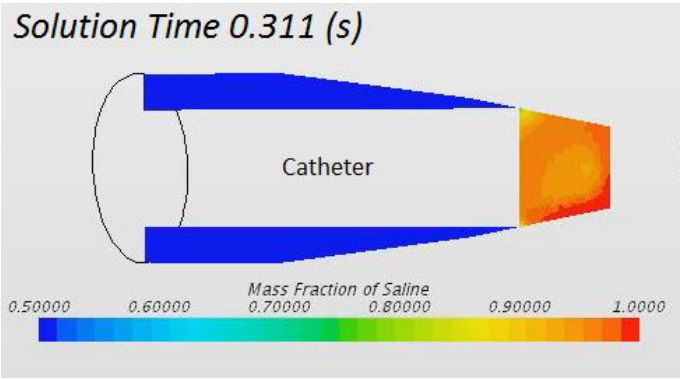

(e)

Figure 5.1 Comparison of flushing times from optical analysis and the qualitative data from simulations. The time of flushing determined from the optical analysis for different cases were compared with the qualitative analyis derived from the simulations. At the prescribed times from the optical technqiue, the simulations showed an orange-dark orange field which signified about 0.95 or 0.96 concentration of saline by mass fraction. This was uniform throughtout different combinations of lumen and plaque geometery.

Clearance of the blood in front of the CTO starts from small regions which grow to clear the entire region as more saline is injected and blood is flushed out. The percentage of this visible area is plotted over time to understand how this region grows. The entire saline flushing process takes between 1 and 3 seconds, however, the clearance action takes place over only about 0.1 seconds. As opposed to a gradual increase in the visibility of the CTO, in particular for the small volumes

generally seen in these procedures, this clearance of blood from zero to hundred percent visibility occurs quickly.

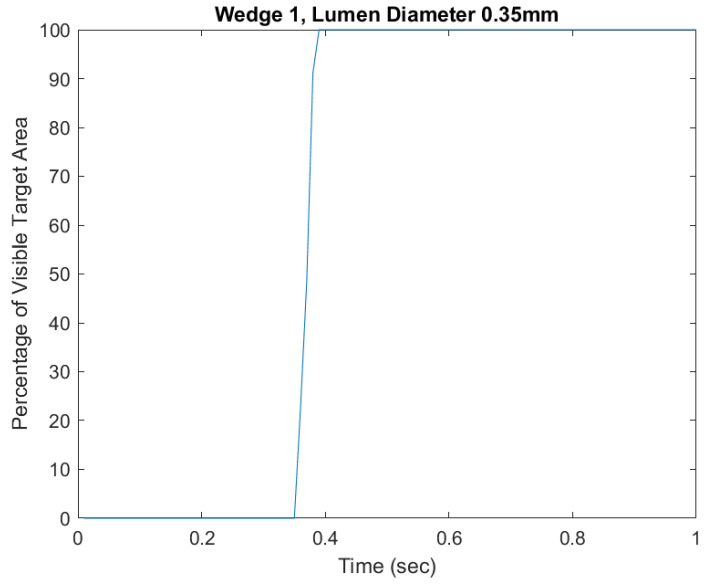

(a)

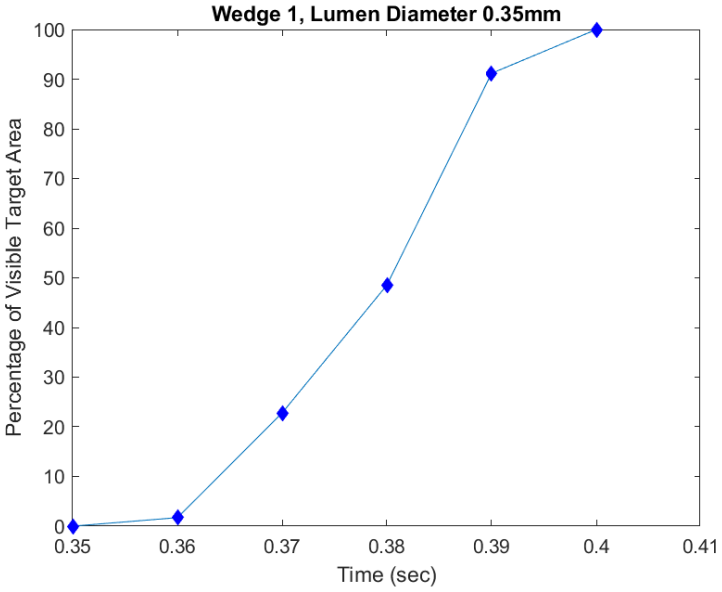

(b)

Figure 5.2 Time dependence of increase in visible area during the saline flushing technique. The clearance of blood takes place within a relatively short time of around 1-2 seconds. However, the increase in the visible area is not instantaneous but grows gradually.

Additionally, the transparency curves for different lumens in catheters are compared across the different catheter designs. The sampling for each of the graphs in Figure 5.3 was done at 0.01 seconds. With a catheter lumen of 0.35 mm diameter, there is a gradual increase in the visible area as saline flushes the blood. However, when the lumen diameter of the catheter is 0.25 mm, there is a sudden increase in visible area from zero to a hundred percentage. This is attributed to the slow accumulation of the saline fluid into a concentrated region in front of the CTO, which crosses the threshold value for visibility suddenly across the entire region as opposed to having a gradually increasing region of visible area.

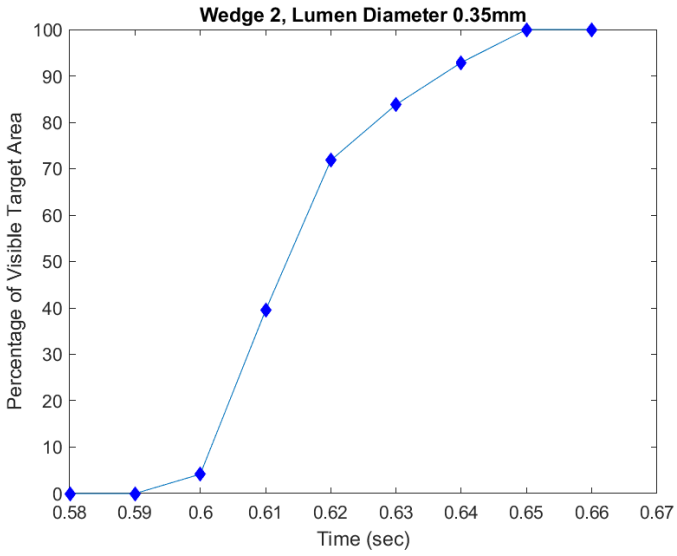

(a)

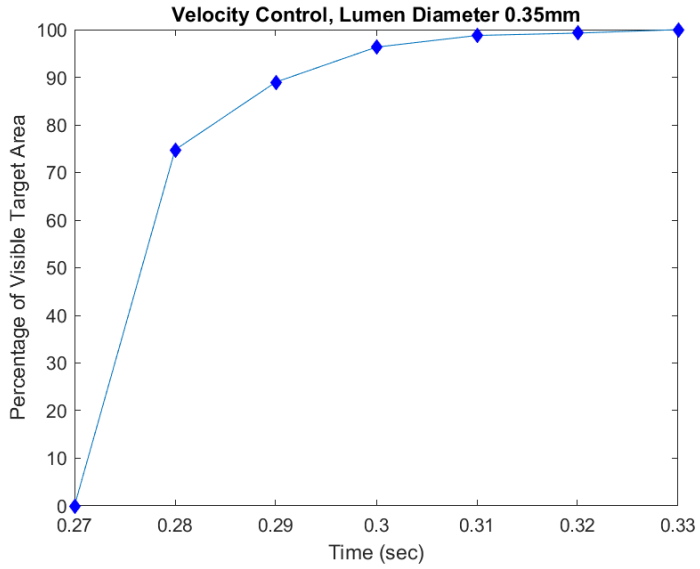
Velocity Control, Lumen Diameter 0.35mm
Percentage of Visible Target Area
Time (sec)
0
10
20
30
40
50
60
70
80
90
100
0.27
0.28
0.29
0.3
0.31
0.32
0.33

(b)

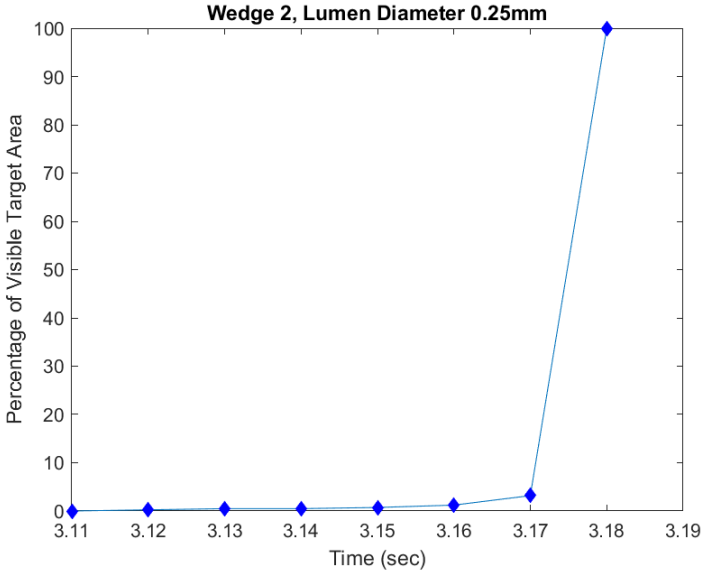
Wedge 2, Lumen Diameter 0.25mm
Percentage of Visible Target Area
Time (sec)
0
10
20
30
40
50
60
70
80
90
100
3.11
3.12
3.13
3.14
3.15
3.16
3.17
3.18
3.19

(c)

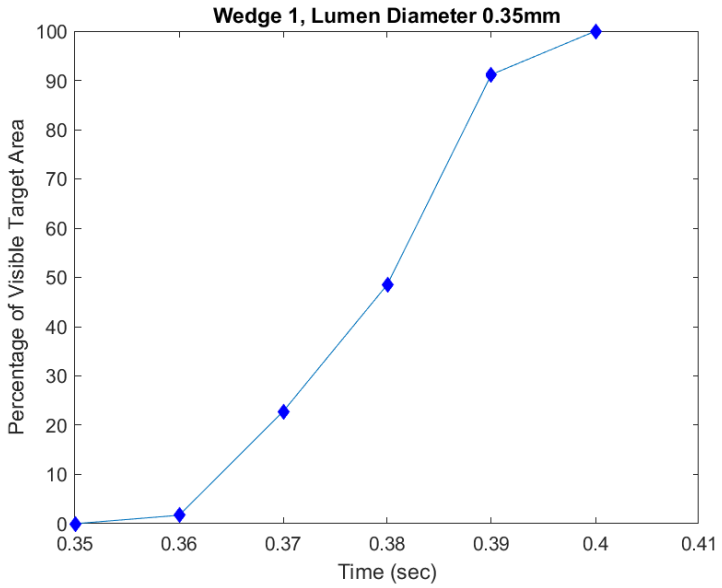

(d)

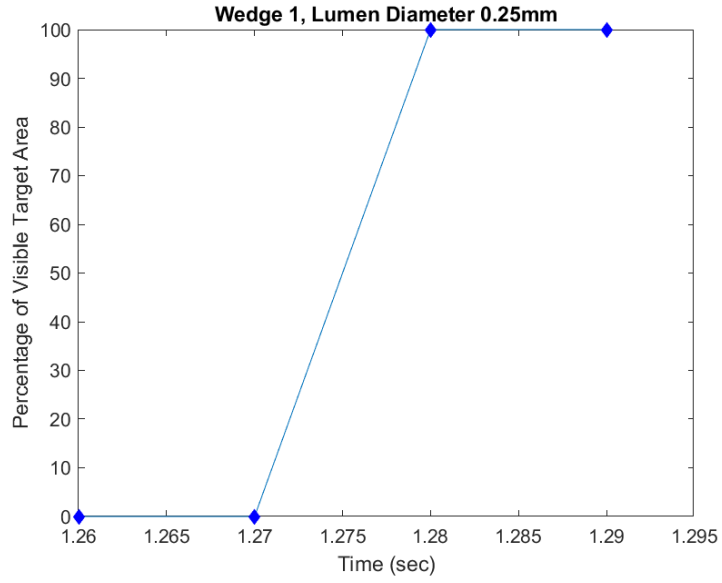

(e)

Figure 5.3 Percentage of visbile target area with time. The optical analysis of different catheter and plaque geometries provided insight into the increase in visibile target area over time during the saline flushing process. The sampling rate for the simulations was 0.01 sec.

For the steep wedge plaque morphology, a change in the lumen diameter from 0.35 mm to 0.25 mm results in an increase in flushing time by a factor of three. In the steeper wedge, the increase

in flushing times by reducing the lumen diameter to 0.25 mm from 0.35 mm is a factor of five. For both plaque morphologies, the time of flushing remains less than a second. By using the larger lumen for suction of saline-blood mixture and injection of saline, flushing times are relatively quick, while representing a reduction of the available area for additional instruments of only 0.1 mm^2. The loss of a small area in the 0.35 mm lumen catheter is well compensated by the gains in the lower flushing times, which would encourage the use of this catheter in practical applications.

In terms of flushing time with respect to volumes, the plaque morphologies each have different clearance volumes due to varying standoff distances between the CTO and the catheter tip. As the clearance volumes increase, the time required to flush the blood increases accordingly. However, there exist significant differences between small and large standoff distances with respect to flushing time. An increase in the clearance volume by a factor of 3.3 results in changing the flushing time by about a factor of five. This suggests it is important to start the saline flushing process while within a suitable distance away from the CTO. The suggested distance is about 2 mm which will result in flushing times of about 1 second in cases where there is limited plaque buildup before the CTO. In cases where a plaque buildup exists in the form of a steep or narrow taper, this will result in even faster clearance helping the interventionist keeping the procedure time within limits.

Morphology	Clearance Volume	Flushing time
Velocity Control (zero clearance between catheter and plaque)	2.011 mm^3	0.300 sec
Steep Taper	3.892 mm^3	0.380 sec
Narrow Taper	6.416 mm^3	0.625 sec
Zero Taper	21.15 mm^3	3.150 sec

Table 5.1 Change in flushing time with clearance volumes. With increasing clearance volumes corresponding to increasing standoff distance the time of flushing increases for a fixed lumen

diameter of 0.35 mm. The recommended standoff distance is about 2 mm which corresponds to volumes in between the steep and narrow taper simulations and flushing times.

CHAPTER 6

CONCLUSIONS AND FUTURE WORK

In this thesis, the fluid mechanics and light physics involved in the saline flushing of blood to visualize CTOs during their treatment have been investigated using computational techniques and ray tracing analysis. The aim of this study is to understand the interaction of blood and saline inside blocked arteries and to improve current treatment methodologies employed, developing new designs for catheters utilized in these procedures.

6.1 Summary of the work

6.1.1 Catheter Design

By using computational techniques, this study shows the evolutionary development of the design of the catheter driven by the fluid dynamics involved in the functionality of the instrument. For each design, the pros and cons are discussed and improvements are introduced to enhance the quality of the catheter and develop a better technique to flush saline inside occluded arteries to visualize and treat CTOs. A simple central channel catheter was first designed, which quickly cleared the blood ahead of the CTO but required large pressures to produce the required saline injection rates. With the center of the catheter occupied, important instruments on the catheter would have to be displaced to other sites on the catheter tip. The design was improved by enlarging the channel area for saline injection, which resulted in lower saline injection pressures that can be accommodated within the diseased artery. The clearance times for blood were within acceptable

levels, but this resulted in the reduction of area available for additional elements of the catheter. On the basis of enhancing the fluid mechanics and circulation utilizing the full effect of the flow patterns that can be generated inside the artery, a suction lumen was introduced diametrically opposed to the injection channel. The introduction of the suction lumen created a new complexity within the catheter, but provided room to include critical instruments needed to treat the CTO. The pressures required to inject saline and collect the saline blood mixture were within safe levels. A further improvement in the design of the catheter was made by shifting the suction and injection lumens adjacent to each other, thus enabling a better area for housing additional elements of the catheter. Finally, the regulation of the saline injection and suction techniques was visited in cases where little or no knowledge of the stand-off distance is available to the clinician. In such cases, a small region of extreme over pressure can be generated while injecting saline in the pressure-regulated mode, which can result in damage or rupture of the weakened artery. A significant improvement was made by switching the suction and injection controls to be based on the mass flow rates as opposed to pressure. By synchronizing the flow of fluids to and from the small cavity, the pressures developed were well within the normal blood pressure limits of the coronary artery, hence avoiding any possible risk of complications that may arise by the technique. The synchronized suction injection was able to provide clearance when the standoff distance increased however the flushing times were increased by 0.6 sec which needs to be taken into consideration.

6.1.2 Feasibility in Diverse Morphologies

In the second study of this thesis, the functionality of catheters is investigated in different arterial morphologies. There exists great diversity in the human circulatory system, particularly in the shape and sizes of the different blood vessels. Additionally, atherosclerotic plaque is developed in a large diversity of shapes within the coronary arteries. The stenosis of arteries leads to formation

of CTOs which need to be treated medically to improve the health of the diseased individual. To verify the functionality of the proposed catheter designs in these different conditions, the catheters were simulated with varying geometric conditions of the arteries and the plaques. As the artery size varies in patients, simulations were conducted to understand the effect of artery size on the saline flushing mechanics. As the clearance between the catheter lateral wall and artery membrane reduces, saline injected into the artery does not penetrate the blood ahead of the CTO. In the absence of a suction lumen, the blood remains unaffected by the momentum of the saline injection and clearance takes place slowly between the catheter and the CTO. To overcome this, a characteristic curve was developed which suggested the optimal clearance time is achievable in suction-less catheters if the catheter diameter is nearly half the diameter of the artery. To test the capability of the technique in actual sections of the coronary arteries, a simple curved model was simulated. The curvature in the artery created a curvature in the catheter itself, resulting in the development of different flow patterns in front of the catheter tip where a significant amount of saline was unutilized in flushing blood away from the CTO. To simulate treatments where a balloon is not used in the catheterization to avoid damage to blood vessel walls, external heart blood pressure was introduced. Blood pumped by the heart affects the pressure distribution within the artery and increase the pressure at which saline needs to be injected to overcome the flow of blood. There are significant differences in the clearance time when the injection timing is varied with respect to the pulsatile blood flow, which may be of use when synchronizing injection of saline with the heartbeat, but are otherwise small. To understand how different plaque morphologies can affect the flushing of blood, simulations with different tapers of plaque development were incorporated. Of the three morphologies studied, namely, steep taper, shallow taper, and negligible taper, the flushing times remain largely within acceptable limits. In one

condition, the clearance time tripled, which is attributed to the large volume between the catheter tip and the CTO. To overcome the increase in flushing time, it is recommended to reduce the standoff distance between the CTO and the catheter tip.

6.1.3 Optical Analysis

In the third part of this thesis, the optical analysis performed provides confidence in the simulations of different catheter designs. Earlier, qualitative methods were used to evaluate when clearance was achieved and the blood was effectively flushed. The analysis using ray tracing provides insight into the actual time when clearance is achieved and the CTO is visible to the clinician. In comparison to the simulation analysis, the agreement between the two techniques is good. The mass fraction of saline ahead of the CTO required for its visibility was determined to be >95% as opposed to 98% which was assumed earlier. Amongst different lumen diameters, catheters with 0.35 mm diameter provided better gains with drastically smaller flushing times in comparison to 0.25 mm diameter lumens. The loss of available area on the catheter cross section for imaging optics is negligible and, hence, the larger lumen diameters are recommended to be used in clinical applications. Additionally, the volume of blood between the catheter tip and the CTO greatly affects the time required to flush the blood. By changing the distance between the catheter and the CTO, flushing times can be significantly reduced allowing additional procedures to be performed quickly. The standoff distance recommended by this study is 2 mm, which can accommodate for different plaque development conditions as well as to provide clearance within reasonable time.

For the most part, between different configurations of catheter design and artery-plaque morphologies, the target clearance time within less than 1 second is deemed reasonable and efficient. While certain designs are able to reduce the flushing time to one-tenths of a second, the requirements to achieve this target time, result in unsafe pressures and larger catheter diameters.

Furthermore, the gains in flushing time are largely insignificant when compared to other steps within the treatment procedure. While modern catheter materials are able to withstand high pressures (between 140 kPa to 500 kPa), such high pressure provide a risk for the patient in case of rupture of the catheter lumen or even the weakened artery. The max pressure injected from the different catheter designs was as high as 440 kPa while safe injection rates were close to 20 kPa. The annulus design is capable of low injection pressure due to its larger injection area, while using a velocity controlled adjacent suction resulted in negligible pressure differences within the artery in comparison to regular operating pressures. The adjacent suction injection lumen designs have a balanced injection pressure requirement of about 90 to 100 kPa. The study suggests pressures close to 100 kPa in injection and about 15 kPa within the artery as safe pressures for the system to be under during the entire procedure. As mentioned earlier, saline flushing is only the initial step in the diagnostic and treatment procedure of the CTO. In addition, elements are required that will help the clinician to operate and clear the blockage assisted in part by the additional visibility due to the catheter designs recommended by this thesis. Hence, the catheter design must have ample room to house elements required to treat the CTO. While the annulus design is hydrodynamically advantageous, it has less than half the area available for additional elements in comparison to a large number of catheter designs. This will result in higher complexity of the instrument while introducing further complications in the manufacture of such devices. This study suggests a reasonable target area for housing the auxiliary apparatus on the face of the catheter to be about 2 mm^2. To accommodate for the space, pressure and time requirements, the study suggests the use of the adjacent suction-injection catheter with a mass flow control assistance to reduce the risk involved in treating CTOs as well as optimizing the entire saline flushing technique associated in this procedure.

6.2 Recommendations of Future Work

6.2.1 Simulation Accuracy

The simulations conducted in the study required to accept a number of general assumptions to provide a basic understanding of the flow mechanics involved during saline flushing of blood. Firstly, the blood mechanics need to be carefully incorporated in simulations. While blood generally acts as a non-Newtonian fluid, in large arteries such as the coronary artery it is safe to assume that blood behaves in a Newtonian fashion. However, when saline interacts with blood and begins to dilute it, the properties of blood change. Blood is a non-homogenous fluid formed by different species including RBC, leukocytes, platelets and plasma. The CFD simulations simplify the physical nature of the blood and model it as a homogenous fluid that mimics water-like properties. These properties in reality are also subject to change as saline interacts with the blood. This study ignores the change in fluid properties of blood as it is diluted and flushed which may introduce a possible error in comparison to the real treatment technique. By incorporating the dynamic variation of the fluid properties of blood the accuracy of these simulations can be improved. Secondly, as mentioned previously, coronary arteries form a complex shape as they reach across the heart to provide blood to the cardiac tissue. The morphology of these arteries is extremely tortuous and the complex nature of these arteries is a fundamental factor in causing heart disease in them. In this study, the complexity of these arteries isn't captured completely. By using simplistic models for the different morphology, insight is gained into the flow structures that are developed. However, as the complexity in the geometry increases the clearance time can be affected, especially in catheter models where an outflow lumen is absent. In such conditions, the saline blood mixture flows outside the clearance zone into the space present between the arterial walls and the catheter, which can alter flushing times, as seen in the curved artery model. Adopting

realistic geometries of the arteries will enhance the results of the simulations. Finally, the walls of the artery have elastic properties to accommodate the pulsatile nature of blood pumped from the heart. The arteries are capable of expanding and contracting in response to the pressure developed inside them. As saline is injected into the heart, the pressure increases across the entire domain. This increase in pressure will result in the expansion of the artery and lead to a change in the volume between the catheter and the CTO. As the volume in the region of interest increases, the required clearance times will change. Similar to the effect of external blood pressure arising from the action of the heart, which affects the injection flow rates of saline, the geometry of the artery will be influenced. The compliance of the arterial wall is a complexity that continues to be challenge computational mechanics simulations (FSI), and can help simulations move closer to actual physical scenarios. By incorporating the wall compliance, a small yet significant difference may take place in the flushing mechanics. However, this comes with an increase in the cost of setting up and running the simulations, due to the complexity of finding constitutive equation and values for the healthy or diseased arterial walls, as well as to determine displacement boundary conditions.

6.2.2 Improvement of the Optical Analysis

The optical analysis in the study establishes the possibility of achieving clearance using different catheter designs. However, there are a few assumptions involved in this study. First, the ray of light incident onto the blood saline mixture and the CTO will undergo continuous scattering by the different species that constitute the blood as it moves through the media to reach the blockage. Upon reaching the CTO, as known using the laws of radiation, a portion of the light is absorbed and reflected and the rest is transmitted. The study assumes 100 percent reflection of light from the CTO, as well as ignores the effect of the angles of reflection that exist in the actual

phenomenon. For simplification, all light incident on the CTO is assumed to return back to the optical receiver. The study also assumes scattering of light due to different species present within the blood to be approximated by an optical density of the medium. Blood is a non-homogenous fluid that contains different particles from RBCs to platelets, each lying within a wide range of sizes and densities. The scattering of light is influenced by each such particle individually within the blood again driven by the basic light absorption, reflection and transmittance formula. The analysis utilizes data derived from previous studies for determining the optical density of blood as a function of hematocrit for different wavelengths of light. In this analysis, wavelength corresponding to green light was selected, which may not be the case in actual clinical applications. The threshold value for visibility was also determined to be 80 percent, which is a decision made using subjective analysis of the target area. At this threshold value, it is deemed that the neighboring blue and white boxes on the target area are clearly distinguishable. As the actual wavelength of light used in clinical applications is considered, the values of the threshold could change and affect the results of the optical analysis. Finally, the ray tracing in this study uses a simple formula where the transmittance is directly related to the mass fraction of saline via the hematocrit. Inside the cone of view, discrete ray paths are drawn from the point of origin to the CTO. This path is divided into discrete zones, where the optical density is evaluated and the combined to determine the total optical density of the light. In reality, light doesn't interact with the media along discrete zones. It undergoes continuous absorption, reflection and scattering as it moves through blood. The analysis also has a finite number of path lines originating from the catheter axis (where the optical fiber is assumed to be placed) towards the CTO. In actual light physics, there are infinite path lines that exist that cover the entire target area. Furthermore, the study uses a single point for the origination of light and receives light reflected by the CTO at the

same point. In most applications, an optical fiber carries light from the external source located outside the catheter and transmits light to the region of interest, while an additional optical fiber carries light back to the display unit located in the operating room. The study assumes, for the sake of simplicity, that both these fibers are superimposed as well as a have radius that can be interpreted as a single point on the tip of the catheter.

6.2.3 Validation of Numerical Simulations

The study focuses on the use of numerical simulations to provide understanding into the flow physics in the technique of saline flushing used to treat CTOs. Numerical simulations involve the solving of physical equations based on appropriate selections of physical models using applied initial and boundary conditions. This entire process is a theoretical methodology whose accuracy depends on the appropriateness of the models selected to solve the problem. These simulations need to be validated using data determined from experiments or actual patient treatments to evaluate their degree of accuracy. It is recommended to perform experiments with prototype catheters using designs proposed by this thesis, which can provide greater insight into understanding the flow physics. This experimental data provides room to improve the simulations by tweaking control points and obtain accurate results on the flushing technique. This approach provides the right venue to test the proposed catheter designs and improve them in the prototype stage of their development before they can be manufactured for clinical applications.

BIBLIOGRAPHY

1. Mozaffarian, D., Benjamin, E. J., Go, A. S., Arnett, D. K., Blaha, M. J., Cushman, M., ... & Huffman, M. D. (2015). Heart disease and stroke statistics—2015 update: a report from the American Heart Association. *Circulation*, *131*(4), e29-e322.
2. https://www.heart.org/en/health-topics/consumer-healthcare/what-is-cardiovascular-disease(Accessed on 10/25/18)
3. https://www.baylorhearthospital.com/Coronary-Artery-Chronic-Total-Occlusion.html (Accessed on 10/25/18)
4. Sianos, G., Morel, M. A., Kappetein, A. P., Morice, M. C., Colombo, A., Dawkins, K., ... & Serruys, P. W. (2005). The SYNTAX Score: an angiographic tool grading the complexity of coronary artery disease. *EuroIntervention*, *1*(2), 219-227.
5. TIMI Study Group*. (1985). The Thrombolysis in Myocardial Infarction (TIMI) trial: phase I findings. *New England Journal of Medicine*, *312*(14), 932-936.
6. Fefer, P., Knudtson, M. L., Cheema, A. N., Galbraith, P. D., Osherov, A. B., Yalonetsky, S., ... & Sparkes, J. D. (2012). Current perspectives on coronary chronic total occlusions: the Canadian Multicenter Chronic Total Occlusions Registry. *Journal of the American College of Cardiology*, *59*(11), 991-997.
7. https://www.mayoclinic.org/diseases-conditions/heart-disease/symptoms-causes/syc-20353118 (Accessed on 10/25/18)
8. Lee, C. M., Engelbrecht, C. J., Soper, T. D., Helmchen, F., & Seibel, E. J. (2010). Scanning fiber endoscopy with highly flexible, 1 mm catheterscopes for wide-field, full-color imaging. *Journal of biophotonics*, *3*(5-6), 385-407.
9. Savastano, L. E., Zhou, Q., Smith, A., Vega, K., Murga-Zamalloa, C., Gordon, D., ... & Thompson, B. G. (2017). Multimodal laser-based angioscopy for structural, chemical and biological imaging of atherosclerosis. *Nature biomedical engineering*, *1*(2), 0023.
10. Engelbrecht, C. J., Johnston, R. S., Seibel, E. J., & Helmchen, F. (2008). Ultra-compact fiber-optic two-photon microscope for functional fluorescence imaging in vivo. *Optics express*, *16*(8), 5556-5564.
11. Savastano, L. E., & Seibel, E. J. (2017). Scanning Fiber Angioscopy: A Multimodal Intravascular Imaging Platform for Carotid Atherosclerosis. *Neurosurgery*, *64*(CN_suppl_1), 188-198.
12. Patel, V. G., Brayton, K. M., Tamayo, A., Mogabgab, O., Michael, T. T., Lo, N., .s.. & Banerjee, S. (2013). Angiographic success and procedural complications in patients undergoing percutaneous coronary chronic total occlusion interventions: a weighted meta-analysis of 18,061 patients from 65 studies. *JACC: Cardiovascular Interventions*, *6*(2), 128-136.
13. Kalniņš, A., Strēle, I., Kurcalte, I., Lejnieks, A., & Ērglis, A. (2018, February). Chronic Total Coronary Artery Occlusion Recanalisation with Percutaneous Coronary Intervention—Single Centre 10-Year Experience. In *Proceedings of the Latvian Academy*

of Sciences. Section B. Natural, Exact, and Applied Sciences. (Vol. 72, No. 1, pp. 1-8). De Gruyter Open.

14. http://www.heartandstroke.ca/heart/treatments/surgery-and-other-procedures/percutaneous-coronary-intervention (Accessed on 10/25/18)
15. https://www.massgeneral.org/heartcenter/services/procedure.aspx?id=2308 (Accessed on 10/25/18)
16. Suero, J. A., Marso, S. P., Jones, P. G., Laster, S. B., Huber, K. C., Giorgi, L. V., ... & Rutherford, B. D. (2001). Procedural outcomes and long-term survival among patients undergoing percutaneous coronary intervention of a chronic total occlusion in native coronary arteries: a 20-year experience. *Journal of the American College of Cardiology*, *38*(2), 409-414.
17. Fernandez, J. P., Hobson, A. R., McKenzie, D., Shah, N., Sinha, M. K., Wells, T. A., ... & O'Kane, P. D. (2013). Beyond the balloon: excimer coronary laser atherectomy used alone or in combination with rotational atherectomy in the treatment of chronic total occlusions, non-crossable and non-expansible coronary lesions. *EuroIntervention: journal of EuroPCR in collaboration with the Working Group on Interventional Cardiology of the European Society of Cardiology*, *9*(2), 243-250.
18. Kawase, Y., Hoshino, K., Yoneyama, R., McGregor, J., Hajjar, R. J., Jang, I. K., & Hayase, M. (2005). In vivo volumetric analysis of coronary stent using optical coherence tomography with a novel balloon occlusion-flushing catheter: a comparison with intravascular ultrasound. *Ultrasound in Medicine and Biology*, *31*(10), 1343-1349.
19. Shen, Z. J., García-García, H. M., Schultz, C., van der Ent, M., & Serruys, P. W. (2010). Crossing of a calcified "balloon uncrossable" coronary chronic total occlusion facilitated by a laser catheter. *International journal of cardiology*, *145*(2), 251-254.
20. Stone, G. W., Kandzari, D. E., Mehran, R., Colombo, A., Schwartz, R. S., Bailey, S., ... & Selmon, M. (2005). Percutaneous recanalization of chronically occluded coronary arteries: a consensus document: part I. *Circulation*, *112*(15), 2364-2372.
21. Yamaguchi, T., Terashima, M., Akasaka, T., Hayashi, T., Mizuno, K., Muramatsu, T., ... & Takayama, T. (2008). Safety and feasibility of an intravascular optical coherence tomography image wire system in the clinical setting. *American Journal of Cardiology*, *101*(5), 562-567.
22. Selmon, M. R., Hansen, G., & Milo, C. (2000). *U.S. Patent No. 6,010,449*. Washington, DC: U.S. Patent and Trademark Office.
23. Levatter, J. I. (2006). *U.S. Patent No. 7,125,404*. Washington, DC: U.S. Patent and Trademark Office.
24. Kittrell, C., Cothren Jr, R. M., & Feld, M. S. (1990). *U.S. Patent No. 4,913,142*. Washington, DC: U.S. Patent and Trademark Office.
25. Abela, G. S. (1991). *U.S. Patent No. 5,041,109*. Washington, DC: U.S. Patent and Trademark Office.
26. Leckrone, M. E., Kagan, J., Knight, D. A., & Gunseor, L. A. (1991). *U.S. Patent No. 5,026,367*. Washington, DC: U.S. Patent and Trademark Office.
27. Winston, T. R., & Neet, J. M. (2000). *U.S. Patent No. 6,106,515*. Washington, DC: U.S. Patent and Trademark Office.

28. Dodge, J. T., Brown, B. G., Bolson, E. L., & Dodge, H. T. (1992). Lumen diameter of normal human coronary arteries. Influence of age, sex, anatomic variation, and left ventricular hypertrophy or dilation. *Circulation*, *86*(1), 232-246.
29. https://www.vitalitymedical.com/guides/urinary/catheter-product-comparison-and-sizing-guide (Accessed on 10/25/18)
30. Guyton, A. C., & Hall, J. E. (1992). Human physiology and mechanisms of disease.